Biomass Conversion and Biorefinery (2023) 13:755–775
https://doi.org/10.1007/s13399-020-01185-z

ORIGINAL ARTICLE

Torrefaction of oil palm empty fruit bunch pellets: product yield, distribution and fuel characterisation for enhanced energy recovery

Bemgba B. Nyakuma[1] · Olagoke Oladokun[1] · Syie L. Wong[1] · Tuan Amran T. Abdullah[1,2]

Received: 20 August 2020 / Revised: 26 November 2020 / Accepted: 1 December 2020 / Published online: 6 January 2021

Abstract

In this study, the non-oxidative torrefaction of oil palm empty fruit bunch (OPEFB) pellets was investigated from 250 to 300 °C for 30 min in a horizontal fixed bed tubular reactor. The effects of the selected conditions on the yields, distributions and fuel characteristics of the torrefaction products were examined. The mass or solid yield (M_Y) decreased from 68.1 to 36.2%, whereas the liquid yield (L_Y) and gas yield (G_Y) increased from 19.4–40.1% and 12.5–23.7%, respectively, due to drying, devolatilization and depolymerisation during torrefaction. Physicochemical and calorific analyses showed that the torrefied OPEFB pellets have high carbon but low oxygen contents, which accounts for the high heating values (HHV = 22.83–25.81 MJ/kg). The torrefied OPEFB pellets also exhibit lower moisture (2–4%) and volatile matter (34.38–65.31 wt.%) but high ash (4–20 wt.%) and fixed carbon (28.69–41.62 wt.%) compared to the raw pellets. The OPEFB pellet fuel properties, namely pH that ranged from 6.65 to 7.74, hydrophobicity from 100 to 23.04% and grindability from 53.66 to 108, were markedly enhanced after torrefaction at 300 °C. The L_Y consisted of organics (67.64–62.62%) and water (32.36–37.38%) fractions characterised by high acidity (pH = 2.89–3.22) and dark hues formed by holocellulose and lignin thermal degradation at higher torrefaction temperatures. Based on the findings, the torrefied OPEFB pellets is a highly grindable, hydrophobic, thermally stable and promising solid biofuel for firing, co-firing or substituting coal in power plants provided the existing challenges that affect global biomass supply chains are addressed in detail.

Keywords Torrefaction · Oil palm wastes · Empty fruit bunches · Pellets · Biomass · Valorisation

1 Introduction

The African oil palm tree (*Elaeis guineensis* Jacq.) is widely cultivated in tropical nations such as Malaysia and Indonesia for the extraction of crude palm oil (CPO) and palm kernel oil (PKO) [1, 2]. Globally, CPO is an essential edible vegetable oil, food ingredient, as well as an industrial raw material for the production of biofuels, biodiesel, biochemicals and biomaterials [3, 4]. Over the years, the demand for CPO has soared geometrically with Malaysia currently accounting for over 30% of the global vegetable oil market [1, 5]. According to the Malaysian Palm Oil Board, the production of CPO in 2018 stood at 19.52 million tonnes, whereas the trade in palm oil-related products amounted to 24.88 million tonnes valued at RM67.5 billion (US$16.37 billion, Exchange rate US$1 = RM4.12) [6]. Likewise, the Agency for Innovation in Malaysia (AIM) estimates that the palm oil industry accounts for over RM80 billion (US$19.40 billion, Exchange rate US$1 = RM4.12) or ~ 8% of the nation's gross national income (GNI) [7].

Despite the significant socio-economic contributions of the industry, the rapid expansion of oil palm tree cultivation and CPO production has created major solid waste disposal and management problems. Typically, the palm oil industry generates over 100 million tonnes of dry solid biomass wastes annually [7] from over 426 palm oil mills in the country [8]. The solid oil palm wastes (OPW) broadly consists of plantation wastes (trunks, fronds and leaves) and the palm oil mill wastes (empty fruit bunches, mesocarp fibres and kernel shells) [9, 10].

✉ Bemgba B. Nyakuma
bbnyax1@gmail.com

✉ Tuan Amran T. Abdullah
tuanamran@utm.my

[1] School of Chemical and Energy Engineering, Faculty of Engineering, Universiti Teknologi Malaysia, 81310 Skudai, Johor, Malaysia

[2] Centre of Hydrogen Energy, Institute of Future Energy, Universiti Teknologi Malaysia, 81310 Skudai, Johor, Malaysia

Current strategies for ameliorating the challenges of the OPW include application as organic manure, mulching material and liming additives to replenish the plantation land [11, 12]. Other studies have reported the open-air burning, landfilling and dumpsite deposition as measures to dispose and manage the growing stockpiles of OPWs [13–15]. However, the outlined disposal strategies are not sustainable due to their potentially damaging effects on human health, safety and the environment. Besides, the continued pursuance of such strategies is likely to exacerbate global warming, climate change and the lingering controversies surrounding the sustainability of the palm oil industry [5, 16]. Given the nature of the following predicaments, the government of Malaysia proposed the National Biomass Strategy (NBS) to sustainably and systematically tackle the nation's soaring stockpiles of OPWs [7]. The policy also seeks to promote the valorisation of 20–32 million tonnes or ~ 30% of all OPWs generated into biofuels, biomaterials, biochemicals and other high-value green products. The long-term objective of the policy is to establish a circular economy from OPW valorisation and promote sustainable energy initiatives that mitigate greenhouse gas emissions [7].

Several challenges have to be overcome to achieve the objectives of the NBS. One of the most critical is the problematic fuel properties of oil palm empty fruit bunches (OPEFB), which is the most abundant solid OPW generated during the production of CPO. OPEFB is the brown, bulky and spikey residue generated after the stripping and processing of the oil palm fruits from the fresh fruit bunches during the CPO production in palm oil mills. Due to its high heterogeneous nature, hydrophilicity, hygroscopicity and susceptibility to microbial degradation properties [10], it is challenging to efficiently transport, dispose, store or manage OPEFB [17]. Likewise, the valorisation of OPEFB is hampered by its high moisture and alkali metal contents along with low heating values, energy density and grindability [18, 19]. Hence, OPEFB requires extensive pre-treatment, processing and conditioning to improve its fuel properties for effective utilisation as raw materials for clean energy and other value-added products [20].

Pelletization has recently been proposed and examined as a promising pre-treatment technique for the densification or compaction of dry, loose, biomass residues into uniform solid structures termed pellets [21]. The use of low-temperature thermal techniques such as torrefaction also improves the fuel properties of biomass feedstock for future applications [22, 23]. Torrefaction is a thermochemical process in which biomass is heated at low temperatures from 200 to 300 °C, short resident times (15–60 min) and heating rates (5–20 °C/min) under inert gas or mildly oxidising environments [24]. During torrefaction, the selected biomass undergoes mild thermal degradation primarily due to dehydration, devolatilization, decarboxylation and depolymerisation reactions. The hemicellulose and partly cellulose and lignin contents are degraded during torrefaction resulting in mass losses (from 5 to 75%), which transforms the atomic ratios and upgrades the fuel properties of the biomass [25–27]. The torrefaction process also improves the grindability, friability, hydrophobicity along with the handling, storage and transportation of biomass [24, 28]. Consequently, the solid torrefied product has higher fuel quality when compared to the raw biomass, as typically examined through the mass yield (M_Y), energy yield (E_Y), higher heating value (HHV), energy density (D_E), torrefaction index (T_I) and severity factor (S_F) of the torrefaction process [29, 30]. Based on the foregoing, torrefaction is considered a pre-treatment as well as valorisation technique, which enhances the fuel properties of hitherto low-quality biomass feedstock for densification, pelletization and power generation through co-firing with coal [31–33]. Torrefaction can also serve as an environmentally friendly and cost-effective approach for the pre-treatment and valorisation of OPW compared to pyrolysis, gasification or combustion [34].

The torrefaction and pelletization of biomass feedstocks, termed the TOP process, has been proposed and extensively examined in the literature [35–38]. However, the TOP process is hampered by numerous challenges. Firstly, torrefaction thermally degrades hemicellulose and lignin, which are responsible for inter-particle cohesion and hydrogen bonding in the biomass structure [39]. The pelletization of torrefied biomass particles without a binder results in poor quality or brittle pellets, which can generate high particulate matter and hazardous off-gas emissions during utilisation and storage [38]. Alternatively, the use of binders increases the moisture and ash content of pellets, which hampers the overall quality of the torrefied pellets. Secondly, the rapid internal diffusion of vapours during torrefaction of biomass particles (< 1 mm) results in poor product yields, higher heating and thermodynamic losses [40]. The pre-treatment and valorisation of oil palm wastes (OPW) are prerequisite processes that enhance energy recovery by thermochemical conversion [40]. Likewise, the combined processes of pelletization and torrefaction can enhance the fuel properties, process efficiencies and energy recovery potential of OPW as a clean fuel for power plants [41].

Uemura et al. [42] showed that the torrefaction of OPEFB from 220 to 300 °C for 30 min produced mass yields of 43–24%, energy yields of 56–83% and higher heating values (HHV) of 17.17–20.41 MJ/kg. Likewise, the torrefaction of palm kernel shells (PKS) produced mass yields of 77–71%, energy yields of 93–100% and HHV of 18.55–21.68 MJ/kg. Asadullah et al. [43] investigated the optimisation and torrefaction of PKS from 200 to 350 °C for 10–60 min. The findings demonstrated that the optimal yields and conditions for PKS torrefaction are mass yield (73%) and higher heating value (24.50 MJ/kg) at 300 °C, 20 min and 300 ml/min. The study also reported the fuel characteristics and distribution of

the solid (mass), liquid and gas products yield of PKS torrefaction, which is lacking in the study on OPEFB by Uemura [42] and other studies on OPEFB in the literature. More recently, Sukiran et al. [22] examined the influences of process parameters on the fuel characteristics of torrefied OPEFB. The findings revealed that the optimal conditions for OPEFB torrefaction were 225 °C, 20 min and 500–700 μm particle size. Similarly, the torrefaction of bamboo (particle size, d = 0.18–0.84 mm) [44], *Leucaena* (d = 0.5–2 mm) [45], wood briquettes [45] and beech wood (d = 2 mm) [46] yield high mass yields (70–96%), energy yields (60–99%) and HHV (18.80–28.50 MJ/kg) under inert (non-oxidative) conditions. The plausible inference is that biomass particle size and chemical structure along with torrefaction temperature, residence time and sweeping gas significantly influence the mass yields, energy yields, process efficiency and the quality of torrefied biomass products.

Despite the numerous publications on the non-oxidative torrefaction of oil palm biomass, there are limited studies on the torrefaction of OPEFB pellets in the literature. Furthermore, existing studies are limited to the pulverised OPW and OPEFB with particle sizes below 1 mm, which result in low yields and distribution of torrefaction products. The research works of Uemura et al. [42] and recently Sukiran et al. [22] are also limited to the effects of torrefaction parameters on the mass and energy yields of pulverised OPW. Hence, the detailed characterisation of the fuel properties such as pH, microstructure, mineralogy, hydrophobicity, grindability, thermal degradation behaviour and characteristic temperature profiles of pelletized OPEFB remains lacking in the literature. Comprehensive fuel and energy characterisation is not only critical to evaluating the energy recovery, market viability and ancillary potential applications of torrefied biomass pellets but also addressing the outlined problems of pulverised biomass torrefaction.

Therefore, this study seeks to investigate the non-oxidative torrefaction of OPEFB pellets as an effective approach for the pre-treatment and valorisation of OPEFB. The OPEFB pellets are thus subjected to non-oxidative torrefaction under the conditions; temperatures, T = 250 °C, 275 °C, 300 °C, atmospheric pressure and residence time, t = 30 min using a horizontal fixed bed tubular (FBT) reactor. The product yield, distribution and fuel characteristics of the torrefied OPEFB pellets and liquid products are subsequently characterised to extensively examine the microstructure, morphology, hydrophobicity, grindability, thermal fuel properties along with the pH and chemical composition, respectively. The study also presents the market dynamics, potential applications and future economic outlook on the torrefied OPEFB pellets based on the fuel characteristics, as extensively detailed in Section 4. To the best of the authors' knowledge, this study is the first comprehensive study on the product yield, distribution and fuel characterisation of torrefied OPEFB pellets under non-oxidative torrefaction conditions in the literature. It is envisaged that the results provide in-depth knowledge on the thermal pre-treatment, pelletization and valorisation of OPEFB as proposed in the NBS-2020 strategy of Malaysia. Lastly, the findings also present solutions to the outlined problems of the TOP process of pulverised biomass torrefaction in the literature.

2 Materials and methods

2.1 Materials

The OPEFB pellets used in this study were purchased from Felda Semenchu palm oil mill located at Kota Tinggi in Johor State of Malaysia. The brown, cylindrically shaped, 8-mm-sized OPEFB pellets (depicted in Fig. 1) on average each weigh about 2.5 g, length of 3 ± 1.5 cm and density of 800 kg/m^3. The OPEFB pellets were manufactured at 60 MPa piston press pressure without the use of binders and were examined in the study without any modification.

Before torrefaction, the OPEFB pellets were characterised to determine the elemental, proximate and HHV properties through ultimate, proximate and higher heating value analyses, respectively. For the tests, the OPEFB pellets were first pulverised in a high-speed crusher (Panasonic Mixer Grinder MX-AC400, Malaysia) and sieved using an analytical sieve (mesh size No. 60, WS Tyler USA) to obtain homogenous particles of size 250 μm.

2.2 Methods

The torrefaction of the OPEFB pellets in this study was performed in a stainless steel tubular reactor horizontal FBT reactor (dimensions length, L = 300 m; diameter, D = 25.4 mm) based on the reactor schematics and set up presented in Fig. 2. The full description of the reactor, schematics and ancillary parts comprising (N_2 gas supply, tubular reactor, Lindberg

Fig. 1 Oil palm empty fruit bunch (OPEFB) pellets

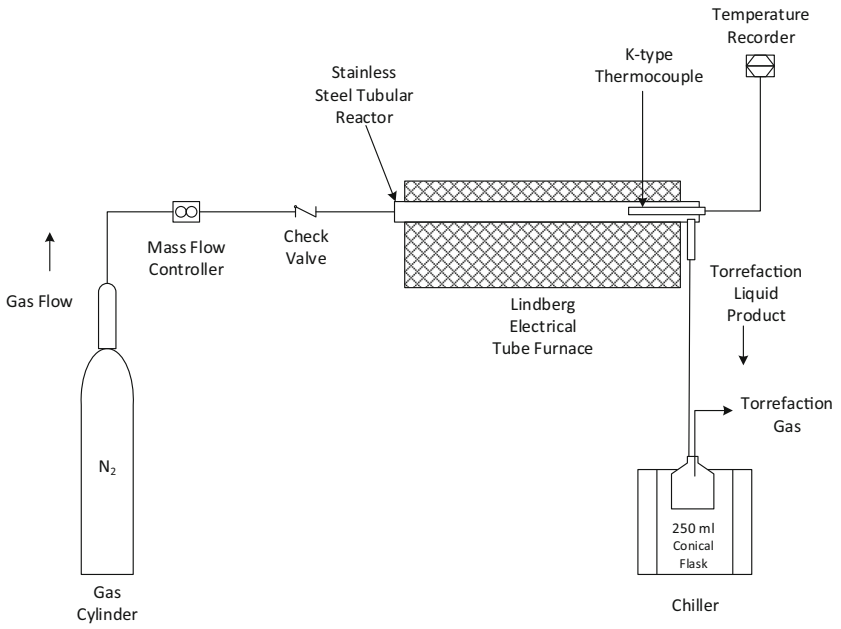

Fig. 2 Schematic of the FBT reactor for OPEFB pellets torrefaction

Furnace, K-type thermocouple and products collection unit) are presented in our previous study [41]. The FBT is a practical, low cost and reliable bench-scale reactor for biomass torrefaction [40].

For each torrefaction test, approximately 15 g of the OPEFB pellets were placed in the stainless steel tubular FBT reactor before transferring to the tube furnace (Lindberg Blue M, USA). The furnace was closed and the entire system purged with the nitrogen gas (N_2, 99.99% purity, Mega Mount Industrial Gases Sdn Bhd, Malaysia) at a flow rate of 200 ml/min for 15 min. The purging process was conducted to create and maintain an anoxic atmosphere for the non-oxidative torrefaction of the OPEFB Pellets. The reliability and accuracy of the purge gas flow rate during the tests was visually verified with a digital flow meter (Altech® DFM 4068, USA). After flushing was completed, the FBT reactor and OPEFB pellets were heated under non-isothermal (dynamic) conditions by ramping from room temperature to the selected torrefaction temperature (T = 250, 275, 300 °C) at a constant heating rate of 15 °C/min. At the selected torrefaction temperature, the isothermal mode was activated and heating was maintained at the selected torrefaction hold time of 30 min. Upon completion of torrefaction, the tube furnace was switched off and the FBT reactor was allowed to cool down to room temperature.

Next, the torrefied OPEFB pellets (solid product) were retrieved, weighed and stored in airtight vessels before characterisation. The torrefaction liquid product was collected in a conical flask (V = 250 ml, Pyrex USA) during torrefaction, after condensing and cooling at 5 °C using a refrigerated bath circulating chiller (Protech 631D, Malaysia). The liquid product was subsequently weighed and stored in airtight sample bottles and placed in a refrigerator at 5 °C before the torrefaction liquid analysis, whereas the torrefaction gas product was flared off during torrefaction. Each test was performed in triplicate to ensure the accuracy and reliability of the measurements. The mass yield (M_Y) of the torrefaction of the OPEFB pellets was computed to determine the energy yield (E_Y) and energy density (D_E) based on Eqs. (1–4) [42, 47, 48]:

$$M_Y = \left(\frac{m_{TB}}{m_{RB}}\right) \times 100 \tag{1}$$

$$E_Y = M_Y \times \left(\frac{HHV_{TB}}{HHV_{RB}}\right) \tag{2}$$

$$D_E = \left(\frac{E_Y}{M_Y}\right) \tag{3}$$

$$S_F = \log\left\{t \times \exp\left(\frac{T_h - T_r}{14.75}\right)\right\} \tag{4}$$

The term m_{TB} represents the mass of torrefied biomass, m_{RB}—the mass of raw biomass (g), M_Y—mass yield (%), E_Y—energy yield (%), D_E—energy density (%), HHV_{TB} (MJ/kg) and HHV_{RB} (MJ/kg) is the HHV for the torrefied and raw OPEFB Pellets, respectively. The term S_F denotes the severity factor, but the S_F terms t, T_h and T_r denote the torrefaction time (min), torrefaction temperature (°C) and reference temperature (100 °C), respectively. The M_Y, E_Y, D_E, HHV and S_F were used to predict the performance of the OPEFB Pellets torrefaction process.

2.2.1 Product yield and distribution

The distribution of the solid (M_Y), liquid (L_Y) and gas (G_Y) products for OPEFB pellets torrefaction in this study were computed from Eqs. 1, 5–7 described in the literature [49, 50]. The solid product or mass yield (M_Y) of OPEFB pellet torrefaction was deduced from Eq. (1), whereas L_Y was deduced from the mass of the liquid collected in the conical flask after torrefaction (Eq. (5)). Lastly, the G_Y was computed from Eq. (6), and the overall product distribution is described by Eq. (7):

$$L_Y, \% = \frac{m_{mass\ of\ liquid\ in\ conical\ flask}}{m_{RB}} \times 100 \quad (5)$$

$$G_Y, \% = 100 - (M_Y + L_Y) \quad (6)$$

$$M_Y + L_Y + G_Y = 100\% \quad (7)$$

It is important to state that although the mass balances for M_Y, L_Y and G_Y sum up to 100%, there may be some losses, as typically observed in such thermal experiments. These losses are considered negligible due to the bench-scale nature, mild operational parameters and small mass of feedstock used during torrefaction [22, 43, 51].

2.2.2 Physicochemical and calorific analyses

The physicochemical analysis of the OPEFB pellets and torrefied OPEFB pellets was determined by ultimate and proximate analyses, together with bomb calorimetry. The ultimate analysis was conducted to determine the elemental Carbon, Hydrogen, Nitrogen and Sulphur (CHNS) composition using the CHNS analyser (vario MACRO cube, Germany). The proximate analysis was conducted to determine the moisture (M), ash (A) and volatile matter (VM) contents based on ASTM standards D3173, D3174 and D3175, respectively, using a muffle furnace (Ney Vulcan D-130, USA). The fixed carbon (FC) was determined by difference from the sum of the M, A and VM. Lastly, the HHV was determined using an oxygen isoperibol bomb calorimeter (IKA C2000, USA).

2.2.3 Morphologic, microstructural and mineralogical analyses

The morphology of the OPEFB pellets and torrefied OPEFB pellets was examined visually to determine the colour changes before and after the torrefaction process. The microstructure and mineralogy were examined through scanning electron microscopy (SEM) and energy dispersive x-ray (EDX) spectroscopy (SEM-EDX JEOL JSM IT 300 LV, Germany), respectively. For each test, the powdered samples were spray deposited on the carbon grain mounts, before being transferred to the sample compartment and degassing in the SEM sample chamber to purge unwanted gases. Next, the samples were scanned in vacuum to acquire the surface micrographs at a magnification of × 1000 through the use of the point ID method. The EDX analysis of the mapped region in the SEM micrograph was simultaneously conducted to quantify the elemental composition of Al, C, Ca, Cl, Cu, Fe, K, Mg, Na, O, P, S and Si in weight percent (wt. %) in the samples based on the EDX peaks and charge balance.

2.2.4 pH Analysis

The OPEFB pellets and torrefied OPEFB pellets were both subjected to pH analysis based on the modified procedure of Rajkovich et al. [52]. Before the tests, the OPEFB pellets and torrefied OPEFB pellets were pulverised and sieved into 250-μm-sized particles. Next, precisely 10 ml of deionised water was added to a 250 ml beaker containing 0.5 g of each pulverised sample based on the ratio of 20:1. The mixture was vigorously stirred at 300 rpm using a magnetic stirrer (Jenway 1103, USA) at room temperature for 90 min. The mixture was filtered using filter paper (Smith A0331, Qualitative 125 mm, UK). The pH of the filtrates was examined on the benchtop pH meter (Martini Instruments Mi-150, USA). Before each test, the pH meter was calibrated with deionised water (pH = 7) at 25 °C, while the pH electrode was cleaned with deionised water after calibration. The pH electrode was then immersed in each filtrate to record the pH.

2.2.5 Hydrophobicity analysis

The hydrophobicity of the OPEFB pellets and torrefied OPEFB pellets were examined based on the modified procedure of Pimchuai et al. [53]. For each test, the OPEFB and torrefied pellets were first weighed and placed in 100 ml ceramic crucibles. Next, 20 ml of distilled water was measured and added to the ceramic crucibles containing the samples before allowing the mixture to stand for 2 h. The samples were then retrieved and weighed to determine the amount of water absorbed. The percentage of water absorbed was calculated from Eq. (8):

$$Water\ Absorbed, \% = \left(\frac{m_{H2O\ absrobed}}{m_{Sample}}\right) \times 100 \quad (8)$$

The terms $m_{H2O,\ absorbed}$ and m_{sample} represent the mass of water absorbed (g) and initial mass of the OPEFB and torrefied pellets (g), respectively.

2.2.6 Grindability analysis

The grindability of the OPEFB pellets and torrefied OPEFB pellets were examined based on the Hardgrove grindability index (HGI_{eqv}) procedure described by Ibrahim et al. [54]. First, the pellets were pulverised and a fixed mass (1.0 ± 0.1

g) of each sample was sieved using the analysis sieve mesh size 200 (Brand: W. S. Tyler USA) to obtain homogenous sized particles below 74 μm. The sample mass (%) that exited the sieve was then weighed and recorded as m_H. The HGI was then computed from Eq. (9):

$$HGI_{equiv} = \frac{m_H + 11.205}{0.4955} \tag{9}$$

The terms HGI_{eqv} and m_H represent the Hardgrove grindability index (HGI) and the mass percentage of products that exited the sieve, respectively. Typically, the lower the HGI value, the harder it is to grind the material [55], and vice versa. Lastly, the HGI values were compared to the grindability scales proposed by Ohliger et al. [46] to examine the effect of the torrefaction process on the grindability of the OPEFB Pellets examined in this study.

2.2.7 Thermal analysis

The thermal reactivity, degradation behaviour and temperature characteristic profiles (TPC) of the OPEFB pellets and torrefied pellets were examined by thermogravimetric analysis (TGA). For each run, about 10 mg of the pulverised (250 μm) torrefied OPEFB pellets were heated in an alumina crucible using the TG analyser (Shimadzu TG-50, Japan) under non-isothermal conditions from 30 to 800 °C at 20 °C/min under air (flow rate 20 ml/min). The objective was to examine the thermal properties under oxidative (combustion) conditions during TGA. On completion, the TG data were retrieved and analysed using the Shimadzu thermal analysis software (Version: TA-60WS workstation) to deduce the mass loss, derivative mass loss and temperature characteristic profiles (TPC). Next, the mass loss (%) and derivative mass loss (%/min) data were plotted against temperature (°C) to obtain thermogravimetric (TG, %) and derivative thermogravimetric (DTG, %/min) plots, respectively, using Microsoft Excel© (version 2013). Based on the TG-DTG plots, the TPCs, onset (T_{onset}), midpoint (T_{mid}), peak decomposition (T_{peak}) and offset (T_{end}) temperatures were deduced from the Shimadzu thermal analysis software. The detailed procedure for determining the TPCs from TG/DTG plots is described extensively in our previous study [56]. The mass loss (M_L, %) and residual mass (R_M, %) were estimated to determine the reactivity and thermal degradation behaviour of the OPEFB and torrefied pellet samples under oxidative (combustion) conditions during TGA.

2.2.8 Torrefaction liquid analysis

The torrefaction liquid products (T_{LQ}) were subjected to colour, pH and water content tests. The objective was to examine its potential footprint, environmental impact or application. For the pH tests, the T_{LQ} samples were transferred to 100 ml beakers for analysis. Before each test, the pH meter was calibrated with deionised water (pH = 7) at 25 °C, and the pH electrode further cleaned with deionised water after the calibration. The pH electrode was then immersed in each T_{LQ} to determine its pH, based on readings recorded using the benchtop pH meter (Martini Instruments Mi-150, USA). Each test was repeated three times to ensure the reproducibility of the measurements. The water content of the torrefaction liquids (T_{LQ}) was examined by Karl Fischer titration (KFT) using the KF titrator (Metrohm AG, 870 KF Titrino plus, Switzerland). The titrator was fitted with a dosing system (Metrohm AG, 800 Dosino, Switzerland) and mixing system (Metrohm AG, 803 Ti Stand, Switzerland). The selected reagent for the volumetric KFT was Hydranal® acquired from Fluka Analytical (Sigma-Aldrich, Malaysia). The data acquisition and handling were performed on the Tiamo™ software (version 1.2). Before each test, the KF titrator was calibrated with deionised water to confirm the reproducibility of the subsequent measurements. For the tests, approximately 0.09 g of sample was measured using a 10 μl syringe (Brand: Hamilton, Switzerland) before injecting into the mixing chamber containing the KF reagent Hydranal for titration. At the titration endpoint, the titre readings were recorded before emptying the vessel through the bottom stopcock connected to the waste bottle. The water content was subsequently calculated from the equation;

$$Water\ content\ (\%) = \left(\frac{KFR_C \times KFR_f}{W_s}\right) \times 100 \tag{10}$$

The terms KFR_c, KFR_f and W_s represent the Karl Fischer reagent consumed (ml) during titration, reagent factor (mg/ml) and sample weight (g), respectively.

3 Results and discussion

3.1 Product yield and distribution

The yields and distribution of the solid, liquid and gas products from the torrefaction of OPEFB pellets are presented in Fig. 3.

The results are based on the average solid mass (M_Y), liquid (L_Y) and gas (G_Y) yields for the OPEFB pellets torrefaction as computed from Eqs. (5)–(7). The results reveal that the solid (mass) yield (M_Y) decreased with increasing torrefaction temperatures from 250 to 300 °C, whereas the liquid (L_Y) and gas (G_Y) yields increased during torrefaction. The decrease in solid (mass) yield (M_Y) from 68.1 to 36.2% can be ascribed to the increased thermal degradation of the lignocellulosic biomass components (e.g. holocellulose, lignin, volatile matter and moisture) of the OPEFB pellets, which

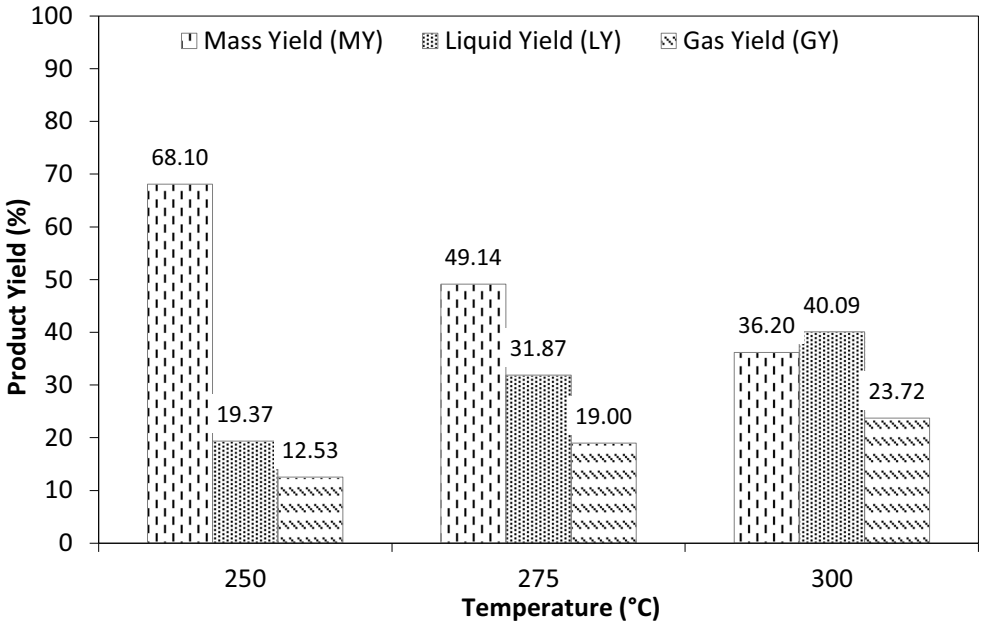

Fig. 3 Product yield and distribution of OPEFB pellets torrefaction

is enhanced at higher temperatures. The drying, devolatilization and depolymerisation of lignocellulosic biomass components during torrefaction account for the decrease in M_Y, which explains the observed increase in the liquid (L_Y = 19.4% to 40.1%) and gas (G_Y = 12.5% to 23.7%). In comparison, the M_Y of the OPEFB pellets reported in this study is significantly higher than the M_Y values (36.98% at 250 °C and 24.18% at 300 °C) reported for pulverised OPEFB [42] and (65% at 275 °C and 55% at 300 °C) for oil palm fibre (OPF) pellets in the literature [57].

The higher yields observed in this study are also ascribed the larger solid uniform size and anisotropic properties of the OPEFB pellets. The size of the OPEFB pellets prevents over oxidation and offers greater resistance to thermal degradation during torrefaction. Hence, the thermal degradation of the OPEFB pellets occurred slowly (i.e. slow pyrolysis) compared to pulverised OPEFB described in Uemura et al. [42] and Chen et al. [57]. Asadullah et al. [43] showed that yield and distribution of products for the torrefaction of palm kernel shell was 60.9% for solid, 24.1% for liquid and 15.1% for gas at 300 °C for 30 min. The findings of this study are in good agreement with Asadullah et al. [43] and other groups in the literature [17, 22, 58, 59] whose findings showed that temperature and particle size markedly affect the yield and distribution of torrefaction products. The higher torrefaction temperatures enhanced the thermal degradation of the lignocellulose (hemicellulose, cellulose and lignin) components of the OPEFB Pellets, thereby resulting in higher mass loss along with lower M_Y but higher L_Y and G_Y (see Fig. 3). Likewise, the small surface area caused by the large particle size, compact and solid uniform nature of the OPEFB pellets slowed the thermal degradation during the torrefaction process. As a result, the residence time for cracking the condensable gases was enhanced thereby resulting in higher G_Y and L_Y.

Next, the torrefaction performance of the process was examined based on the energy yield (E_Y), energy density (D_E), HHV and severity factor (S_F) of the torrefied OPEFB pellets. The parameters were calculated from the mass yields (M_Y) at different torrefaction temperatures, as highlighted in Eqs. (2)–(4). The results for the E_Y, D_E, HHV and S_F for the torrefied pellets are presented in Table 1. The results showed that for all cases, the D_E, HHV and S_F increased, whereas the E_Y decreased with increasing torrefaction temperatures. This observation is attributed to the major decrease in M_Y during OPEFB pellet torrefaction earlier surmised in Fig. 3.

As observed in Table 1, the D_E further increased from 1.29 to 1.47 due to the improvement in the HHV of the torrefied OPEFB pellets from 22.83 to 25.81 MJ/kg compared to 17.57 MJ/kg for the raw OPEFB pellets. The HHV of the torrefied OPEFB pellets (22.83 MJ/kg at 250 °C and 25.81 MJ/kg at 300 °C in this study) is significantly higher than pulverised torrefied OPEFB (17.67 MJ/kg at 250 °C and 20.41 MJ/kg at 300 °C) and torrefied PKS (19.07 MJ/kg at 250 °C and 21.68 MJ/kg at 300 °C) by Uemura et al. [42], while Asadullah et al. [43] reported 21.40 MJ/kg (at 250 °C) and 24.50 MJ/kg at (300 °C) for torrefied PKS. The findings in this study reveal that the HHV of raw OPEFB pellets was significantly enhanced by 20.25–47.18%, which are much higher than reported for other torrefied OPWs in the literature.

The findings confirm that the solid uniform nature of the OPEFB pellets played a significant role in torrefaction. Furthermore, the findings indicate that torrefaction can be employed to effectively upgrade the solid fuel properties of OPEFB for energy and power applications such as co-firing

Table 1 Torrefaction performance and energy efficiency parameters for torrefied OPEFB pellets

Temperature (°C)	Energy yield (E_Y, %)	Energy density (D_E)	Higher heating value (HHV, MJ/kg)	Severity factor (S_F)
OPEFB Pellets	**	**	17.57	**
250	88.49	1.29	22.83	5.89
275	68.80	1.40	24.60	6.63
300	53.17	1.47	25.81	7.37

with coal [31–33]. Lastly, the findings of this study indicate that the S_F improved from 5.89 to 7.37 during torrefaction of the pellets from 250 to 300 °C for 30 min. The severity factor (S_F) is an index used to examine the effect of temperature and residence time on the torrefaction process. In this study, the torrefaction time is fixed at 30 min, hence the increase in the S_F is due to the profound effect of higher temperatures on the process, as computed from Eq. 4. The results are comparable with Lee et al. [60] who reported S_F values from 6.12 to 7.0 and from 5.23 to 7.00 reported by Na et al. [48].

3.2 Physicochemical properties

The physicochemical characteristics of the torrefied OPEFB pellets are presented in terms of the ultimate (elemental), proximate and atomic ratio analyses. Table 2 presents the ultimate analysis and the magnitude of change in the elemental composition of the raw OPEFB pellets and torrefied OPEFB pellets after torrefaction on a comparative basis.

The symbols are defined as C—carbon, H—hydrogen, N—nitrogen, S—sulphur and O—oxygen. The negative signs represent decreases in percentage elemental composition, whereas the positive signs denote increases in the percentage elemental composition after torrefaction. The results demonstrate that the elemental composition of the raw OPEFB pellets was significantly transformed after torrefaction based on the conditions examined in this study. The highest change in the percentage elemental composition was observed for C compared to H, N and O with increasing temperatures during torrefaction. The observed changes can be ascribed to drying, degradation (holocellulose and lignin), decarboxylation and devolatilization of the OPEFB Pellets, which resulted in higher carbon formation, loss of hydrogen and deposition with increasing torrefaction temperatures. The change in the percentage elemental composition of C and O is due to decarboxylation as well as H and O due to drying is responsible for the enhancement of the HHV of the torrefied biomass, as earlier presented in Table 1. However, the minor increase in S observed at 250 °C and subsequent decrease at 275 °C and 300 °C may be due to either sulphurisation or desulphurisation reactions during torrefaction. The minor increase may be due to the formation of hydrogen sulphide (H_2S) from elemental H and S, which occurs at temperatures below 400 °C as reported by Dowling et al. [61]. The decomposition of H_2S at higher torrefaction temperatures [62] may account for the subsequent decrease in S content, as reported in Table 2. Furthermore, the change in percentage elemental composition of the elements C H, N, S and O altered the atomic ratios of the torrefied biomass. Based on the above, the changes in the atomic H/C, O/C, C/N and CH/NS ratios of the OPEFB pellets were examined after torrefaction, as presented in Table 3.

As observed, the H/C and O/C ratios decreased with increasing temperature during torrefaction of the OPEFB pellets. The atomic ratio is a classification tool employed to examine the energy content, potential products and applications of biomass after conversion [24]. The findings of this study indicate that lower H/C and O/C ratios were observed for the torrefied OPEFB pellets compared to the raw OPEFB pellets. This observation is responsible for the higher HHV of the torrefied OPEFB pellets (see Table 1) compared to the feedstock pellets. Similarly, the C/N ratios of the torrefied OPEFB pellets were markedly higher than the raw pellets. The C/N ratio is a measure of carbon to nitrogen in high carbonaceous biomass, which is critical to its utilisation as biochar for soil amendment and other sustainable agriculture applications [63, 64]. As observed in Table 3, the C/N ratio values increased sharply from 37.41 in raw OPEFB pellets to 60.23 after torrefaction at 250 °C but decreased at 275 °C before slightly increasing at 300 °C. Lastly, the CH/NS ratios of the raw and

Table 2 Ultimate analyses of raw OPEFB and torrefied OPEFB pellets

Sample code/temperature	C (wt.%)	ΔC (wt.%)	H (wt.%)	ΔH (wt.%)	N (wt.%)	ΔN (wt.%)	S (wt.%)	ΔS (wt.%)	O (wt.%)	ΔO (wt.%)
OPEFB pellets	41.71	**	5.53	**	1.12	**	0.12	**	51.53	**
250	50.31	8.60	5.38	− 0.15	0.84	− 0.28	0.14	+0.02	43.33	− 8.20
275	58.88	17.17	4.91	− 0.62	1.08	− 0.04	0.10	− 0.02	35.02	− 16.51
300	63.49	21.78	4.41	− 1.12	1.12	0.00	0.10	− 0.02	30.88	− 20.65

Table 3 Atomic ratios of the raw OPEFB and Torrefied OPEFB pellets

Sample code/torrefaction temperature	H/C	O/C	C/N	(CH/NS)
OPEFB pellets	0.130	1.24	37.41	38.38
250	0.107	0.86	60.23	56.89
275	0.083	0.59	54.71	54.16
300	0.069	0.49	56.58	55.56

torrefied OPEFB pellets were examined. The CH/NS presents the ratio of combustible (CH) to pollutant elements (NS) in biomass. The findings of this study demonstrated that the proportion of combustible to pollutant elements in the torrefied pellets is higher than the raw pellets. In general, the increase in temperature improved the CH/NS ratios, which indicates that torrefaction improves the overall fuel properties of the biomass despite the net increase in pollutant content of the elements.

The proximate analysis of the raw OPEFB pellets and torrefied OPEFB pellets are presented in Table 4, based on the moisture (M), volatile matter (VM), ash (A) and fixed carbon (FC) contents. The negative signs represent a decrease in the percentage composition of the torrefied product, whereas the positive signs denote an increase in the percentage composition after torrefaction.

As observed, torrefaction of the raw OPEFB pellets resulted in the loss of M and VM due to drying and devolatilization, respectively. Further analysis revealed that the VM decreased with increasing torrefaction temperature, whereas the M exhibited an opposite trend. The increasing trend in M may be due to the high liquid and condensable products (consisting of water and volatile organics) earlier reported during torrefaction. The plausible reason could be that at higher temperatures, the rate of devolatilization was enhanced, resulting in high liquid products responsible for the trend in M. The FC and ash also increased significantly after the torrefaction process at higher temperatures. The FC is strongly dependent on VM, as such the high content of FC is due to the marked loss of VM during torrefaction [24]. However, the high ash could be attributed to oxidative and exothermic reactions that occurred during torrefaction due to the lignocellulosic and inherent oxygen content of biomass [30, 65, 66]. The observed trend in ash after torrefaction may also be due to the high alkali and alkali earth metals (AAEM). AAEMs are known to catalyse redox or chemical looping reactions during torrefaction, which oxidises the biomass during torrefaction resulting in high ash as also observed in this study. While the nature of such reactions is as yet unclear, most studies also reported high ash after torrefaction [65, 66].

3.3 Microstructural, mineralogical and morphological properties

The microstructural and mineralogical properties of the raw OPEFB pellets and torrefied OPEFB pellets are presented in the SEM/EDX micrographs (at a magnification of × 1000) in Fig. 4. The micrograph of the raw OPEFB pellets in Fig. 4a consists of an irregularly shaped particle morphology that is characterised by a dense network of fibrous materials typically ascribed to the lignocellulosic components (holocellulose and lignin) found in biomasses [56]. The SEM micrograph of the torrefied OPEFB Pellets at 250 °C in Fig. 4b reveals a knaggy fibrous structure characterised by a small network of micropores, as observed on the top left corner of the image. This indicates that the irregular shaped and elongated fibres of the raw OPEFB pellets were partially defibrated, thereby creating the compact structure in the torrefied pellets in Fig. 4b.

The partial defibration and resulting micro-pore formation are due to polymeric hemicellulose degradation during torrefaction [67]. The structure of the torrefied OPEFB pellets at 275 °C in Fig. 4c reveals a network of mesopores and parallel strands of fibres (microfibrils). This observation reveals that the increased severity of torrefaction further degraded holocellulose structures, thereby transforming the micropores into mesopores, which exposed the microfibrils or cellulose fibres observed in Fig. 4c. This confirms that cellulose degradation occurred at 275 °C resulting in the structural modification of the pellets. Likewise, this validates the earlier statement that cellulose degradation accounts for the high liquid products and microstructural changes that enhance the grindability of torrefied biomass [68]. The micrograph of the torrefied OPEFB pellets at 300 °C in Fig. 4d is characterised by a dense network of macropores similar in structure to a beehive or honeycomb. This observation establishes that the degradation of hemicellulose and cellulose was significant, which eliminated the mesoporous and microporous fibres

Table 4 Proximate analyses of raw OPEFB and Torrefied OPEFB pellets

Sample code/torrefaction temperature	M	ΔM	VM	ΔVM	A	ΔA	FC	ΔFC
OPEFB Pellets	7.78	**	75.19	**	5.80	**	11.24	**
250	2.00	− 5.78	65.31	− 9.88	4.00	− 1.80	28.69	17.45
275	3.00	− 4.78	50.52	− 24.67	11.88	6.08	34.60	23.36
300	4.00	− 3.78	34.38	− 40.81	20.00	14.20	41.62	30.38

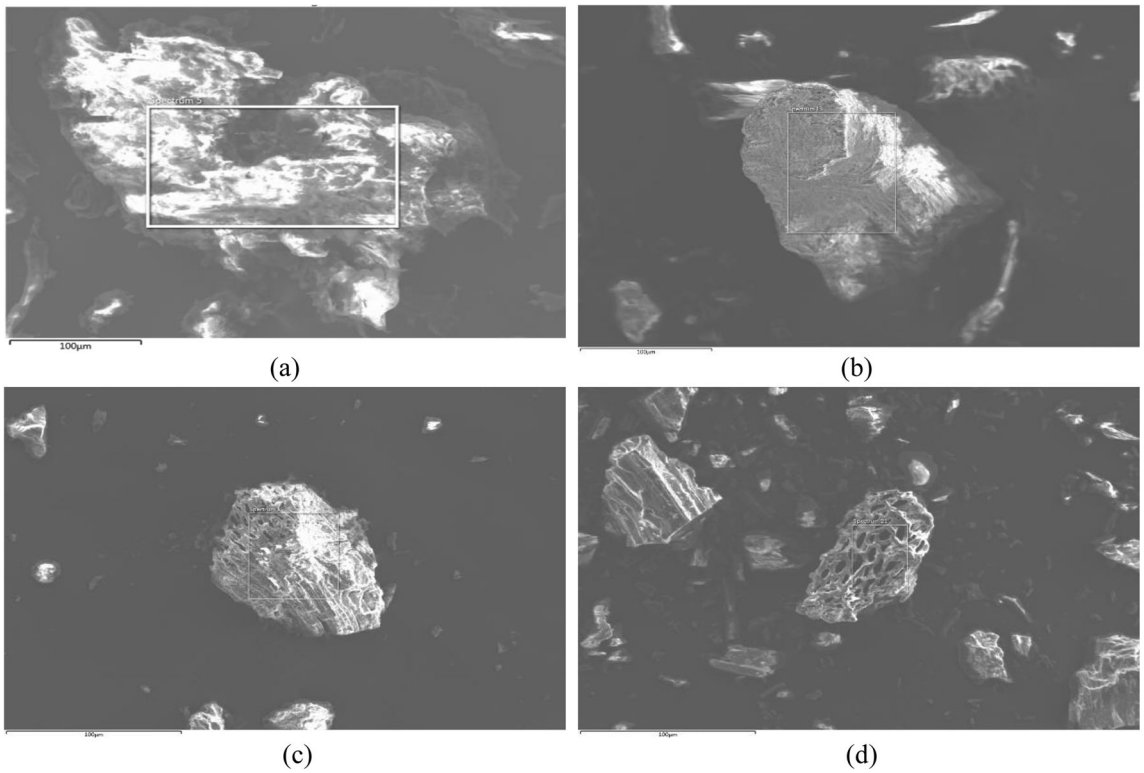

Fig. 4 SEM micrographs of raw OPEFB pellets and torrefied OPEFB pellets. **a** Raw OPEFB pellets. **b** Torrefied OPEFB pellets at 250 °C. **c** Torrefied OPEFB pellets at 275 °C. **d** Torrefied OPEFB pellets at 300 °C

(microfibrils) after torrefaction at 300 °C. Hence, the fuel properties of the OPEFB pellets torrefied at 300 °C will be significantly different from the torrefied OPEFB pellets at 250 °C and 275 °C.

The mineralogical composition of the raw OPEFB pellets and torrefied OPEFB pellets examined by energy dispersive X-ray (EDX) analysis are presented in Table 5. The elements Cu and Na were identified in trace quantities, whereas Al was not detected (ND) after torrefaction at 300 °C. The results reveal that the mineralogical composition of the OPEFB pellets was significantly altered particularly after torrefaction at 300 °C. Therefore, the discussion will be limited to the comparative analysis of the effects of torrefaction on the elemental composition of the raw OPEFB pellets and the torrefied OPEFB pellets at 300 °C. The most significant increase in elemental composition was observed for C, S, K and Cl, whereas Si, O and Ca has the least.

The percentage composition of C increased by 34.83%, whereas S was reduced by 60% after torrefaction at 300 °C. Likewise, the percentage composition of K increased by 267.50%, whereas Cl was by a whopping 310%. The percentage composition of O decreased by 58.04% after torrefaction at 300 °C. The decrease was due to the drying and decarboxylation reactions, which releases H_2O and CO_2 during torrefaction [24]. Hence, the percentage composition of O in the torrefied pellets was lower than the raw OPEFB Pellets. Similarly, the percentage composition of Si decreased from 0.38 to 0.03 wt.% and Ca was from 0.18 to 0.13 wt.% after torrefaction at 300 °C. In summary, the severity of torrefaction conditions considerably changed the mineralogical composition of torrefied biomass compared to the raw OPEFB pellets.

The morphology of raw and torrefied OPEFB pellets was also examined to analyse the physical appearance and colour changes that occurred during torrefaction, as presented in Fig. 5. The colour of the raw OPEFB pellets was transformed from greyish brown to black after torrefaction from 250 to 300 °C. The colour appearance of the raw OPEFB pellets changed progressively with increase in temperature during torrefaction. The observed colour changes are related to the increase in carbon (C) and fixed carbon (FC) composition after torrefaction (see Tables 2 and 4) [42, 43]. At higher torrefaction temperatures, the thermal energy input required for lignocellulosic degradation was enhanced during torrefaction.

3.4 pH of raw and N_2 torrefied pellets

The pH of the raw and torrefied OPEFB pellets was comparatively examined based on the procedure of Rajkovich et al. [52]. The objective of the pH analysis is to evaluate the extent of the torrefaction process on the raw OPEFB pellets and the potential of the torrefied OPEFB pellets for application as biochar. The pH of the raw OPEFB pellet was 6.65, whereas the torrefied OPEFB pellets were 7.62, 7.43 and 7.74 after

Table 5 Mineralogical composition of the raw OPEFB and torrefied OPEFB pellets

Element	Symbol	Composition (wt.%)			
		OPEFB pellets	Torrefied pellets at 250 °C	Torrefied pellets at 275 °C	Torrefied pellets at 300 °C
Aluminium	Al	0.07	0.12	0.12	ND
Carbon	C	57.74	68.24	75.68	79.94
Calcium	Ca	0.18	0.14	0.11	0.13
Chlorine	Cl	0.11	0.10	0.03	0.41
Iron	Fe	Trace	0.02	0.01	0.16
Potassium	K	1.08	0.66	0.68	2.94
Magnesium	Mg	0.10	0.07	0.09	0.08
Oxygen	O	40.13	30.41	22.78	16.09
Phosphorus	P	0.10	0.06	0.03	0.06
Sulphur	S	0.10	0.05	0.05	0.08
Silicon	Si	0.38	0.08	0.42	0.03

torrefaction at 250 °C, 275 °C and 300 °C, respectively. The results showed that the pH increased from weakly acidic (6.70) in the raw OPEFB pellets to weakly alkaline (7.60 on average) after torrefaction. The rise in pH of the torrefied OPEFB pellets could be due to the significant change in elemental (C and H) composition after torrefaction [69, 70]. Sadaka, Negi [27] observed that the pH of torrefied wheat straw increased from 5 to 8 due to the decrease in hydrogen with increasing torrefaction severity, as also observed by other groups in the literature [71, 72]. The increase in pH may also be due to the significantly high content of ash (AC) and fixed carbon (FC) observed in the torrefied pellets (Table 4). Biomass ash typically contains a high content of metals elements and mineral matter [73, 74]. It can be surmised that the

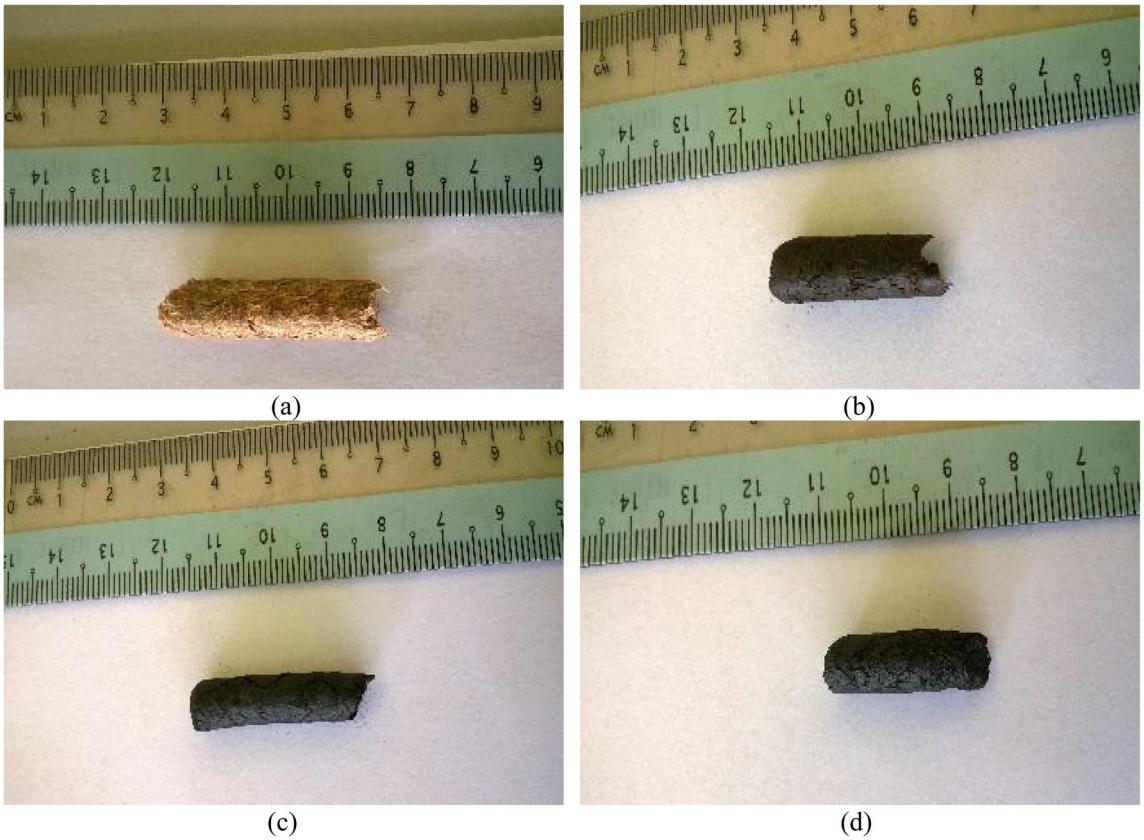

Fig. 5 Colour changes during OPEFB pellets torrefaction. **a** Raw OPEFB pellets. **b** Torrefied OPEFB pellets at 250 °C. **c** Torrefied OPEFB pellets at 275 °C. **d** Torrefied OPEFB pellets at 300 °C

mineral elements in the torrefied pellets formed aqueous alkaline solutions with the torrefaction liquids observed, which explains the increase in pH observed in this study. Based on the alkaline pH, the torrefied OPEFB pellets could be potentially utilised for biochar applications.

3.5 Hydrophobic properties

The hydrophobicity of the raw and torrefied OPEFB pellets was investigated to determine the water absorption before and after torrefaction. Figure 6 presents the structure of the raw OPEFB pellets before and after the hydrophobicity tests.

The solid uniform structure of raw OPEFB pellet was almost completely disintegrated after the 2-h test as observed in Fig 6b. This observation is ascribed to the high uptake or absorption of water, which after percolating the pores of the OPEFB pellets ruptured its solid structure during the tests. Hence, it can be surmised that the raw OPEFB pellets exhibit poor hydrophobic properties. Figure 7 presents the results of the hydrophobicity test for the torrefied OPEFB pellets. In contrast to the raw OPEFB pellets, the structure of torrefied OPEFB pellets remained intact during/after the hydrophobicity tests. The results demonstrate the increased hydrophobicity of the torrefied pellets at elevated temperature. As observed, the torrefied pellet at 250 °C absorbed the highest percentage of water at 56.93%, compared to the samples at 275 °C (35.24%) and 300 °C (23.04%) after the hydrophobicity tests. The findings can be ascribed to the inability of the torrefied pellets to form adequate hydrogen bonds due to loss of OH, which facilitates water uptake or absorption as observed in the raw OPEFB pellets [24]. The results also demonstrated that torrefaction improved the hygroscopic properties of the OPEFB pellets, thus enhancing its overall energy potentials.

3.6 Grindability properties

The grindability of the raw and torrefied OPEFB pellets was examined through the Hardgrove Grindability Index (HGI) [46, 54], as presented in Fig. 8. The grindability of the raw OPEFB pellets increased from 53.66 before torrefaction to 55.94, 69.14 and 108 after torrefaction at 250 °C, 275 °C and 300 °C, respectively. According to Shang et al. [55], the lower the HGI value, the harder it is to grind the material and vice versa. The findings indicate that the grindability of the OPEFB pellets was enhanced with increasing severity of the torrefaction temperatures. This indicates the cost and energy requirements for grinding the pellets will also be significantly reduced after torrefaction. Various studies in the literature have reported similar improvements in the grindability of wheat straw [55], willow, eucalyptus [54] and the grass clippings fraction of MSW [75]. According to the authors, the increase in grindability is ascribed to the depolymerisation of holocellulose and lignin, along with drying and devolatilization reactions, which make the torrefied materials friable or brittle [24]. To verify this, the HGI was compared with the moisture and volatile matter contents of the raw OPEFB pellets and torrefied OPEFB pellets, as presented in Fig. 9.

The plots revealed a linear correlation between the HGI and the physicochemical properties of the raw and torrefied OPEFB pellets. As observed, the grindability of the pellets improved with a decrease in the VM. However, the effect of the increased MC on the grindability of the torrefied OPEFB pellets was insignificant. The plausible inference could be that MC did not affect grindability because the values were lower than the raw OPEFB pellets. Lastly, the relationship between HGI and the properties of fixed carbon and ash showed a linear correlation. Hence, it can reasonably be inferred that the change in fuel properties of the torrefied OPEFB pellets improved the grindability of the torrefied pellets.

(a) (b)

Fig. 6 Hydrophobicity tests for raw OPEFB pellets

3.7 Thermal properties

The thermal degradation behaviour and temperature profile characteristics (TPC) of the raw OPEFB pellets and torrefied OPEFB pellets were examined by thermogravimetric analysis (TGA) as presented in the TG (%) and DTG (%/min) plots in Figs. 10 and 11.

As observed, the raw and torrefied OPEFB pellets experienced significant and progressive mass loss (%) typified by the "double z" or "two-step" downward sloping curves. The TG plots for the torrefied OPEFB pellets also shifted to the right-hand side with increasing severity of the torrefaction temperature. This indicates that the thermal degradation occurred at higher temperatures compared to the raw OPEFB pellets during TGA. This could be attributed to the higher carbon and lower volatile matter (Tables 2 and 4) of the torrefied OPEFB pellets. These two factors also account for the lower thermal reactivity of various solid carbonaceous fuels as observed in coal and petroleum coke during TGA [76–78]. To further examine the reactivity, the characteristic temperature profiles (TPC) for the combustion of the raw and

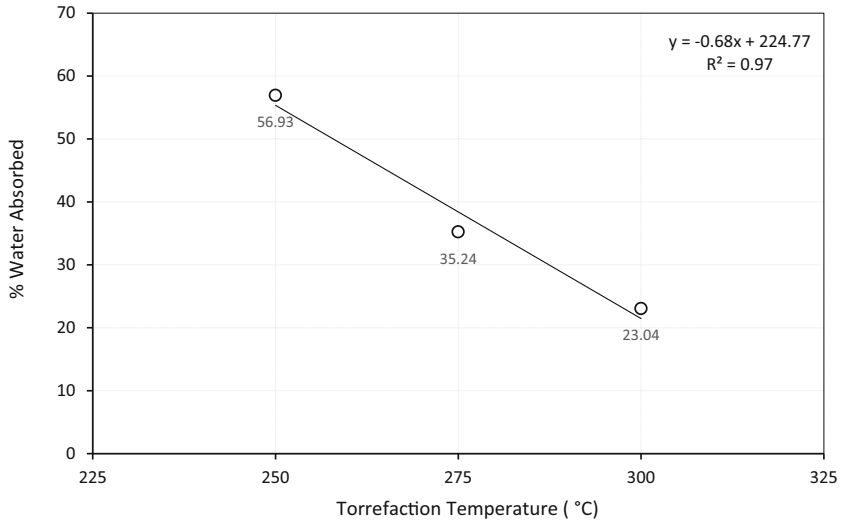

Fig. 7 Hydrophobicity of torrefied OPEFB pellets

torrefied OPEFB pellets were examined and presented in Table 6.

The results indicate that the onset (T_{onset}), offset (T_{end}), mass loss (M_L) and residual mass (R_M) TPCs of the raw OPEFB pellets were significantly altered after torrefaction. The T_{onset} (262.01 °C) of the raw OPEFB pellets increased by 2.67 °C after torrefaction at 250 °C; and 8.53 °C after torrefaction at 275 °C; lastly by 23.49 °C after torrefaction at 300 °C. Similarly, the T_{end} of the OPEFB pellets torrefied at 250 °C, 275 °C and 300 °C were observed at higher temperatures 2.83 °C, 46.20 °C and 148.76 °C, respectively, compared to the raw OPEFB pellets. Based on the T_{onset} and T_{end} of TG plots, the oxidative degradation of the raw OPEFB pellets occurred over a temperature range of 65.96 °C compared to 66.12 °C, 103.63 °C and 191.23 °C for the pellets torrefied at 250 °C, 275 °C and 300 °C, respectively. It can be reasonably surmised that the torrefied OPEFB pellets are more thermally stable or less reactive, which is due to their lower VM contents. Hence, the torrefied OPEFB pellets require higher temperatures, energy input and reaction time to undergo thermal degradation compared to the raw OPEFB pellets. This is confirmed by the mass loss (M_L = 94.90 %) of the raw OPEFB pellets, which is higher than the torrefied pellets (91.50% to 94.24%). Lastly, the residual mass (R_M, %) of the raw OPEFB pellets was lower than the torrefied OPEFB pellets at 5.76% at 250 °C, 7.07% at 275 °C and 8.50% at 300 °C. Next, the reaction pathway and decomposition mechanism of the raw and torrefied OPEFB pellets were examined by the size, shape and symmetry of the DTG plots in Fig. 11.

The DTG plots revealed three sets of decomposition peaks for the raw and torrefied OPEFB pellets. Based on the size, symmetry and position of the DTG peaks, the thermal decomposition occurred in four (4) stages, namely stage I (30–200 °C), stage II (200–325 °C), stage III (325–525 °C) and finally

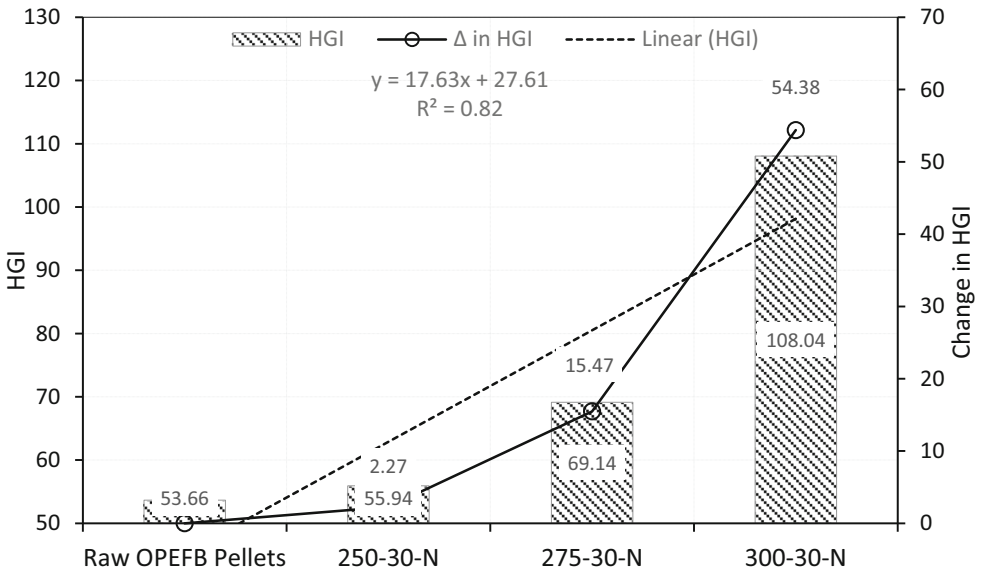

Fig. 8 Grindability of raw and N_2 torrefied OPEFB pellets

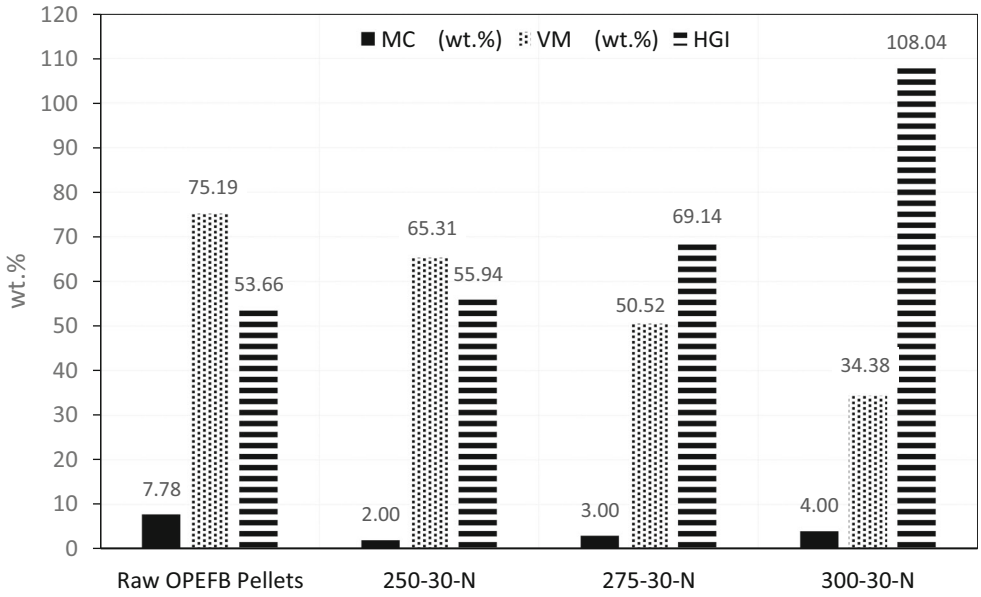

Fig. 9 HGI and fuel properties of raw and torrefied OPEFB pellets

stage IV (525–800 °C). The different stages, I, II, III and IV, can be attributed to drying, devolatilization, char combustion and ash formation, respectively. The most critical stages during the combustion of the raw and torrefied pellets were I, II and III due to the significant mass loss experienced during these stages. The TPCs of the DTG peaks detected in these stages were subsequently analysed to deduce the decomposition mechanisms of the raw and torrefied pellets.

Table 7 presents the TPCs of the raw and torrefied OPEFB pellets deduced from the DTG plots in Fig. 11. The peak temperatures for stages I, II and III during TGA are denoted as T_{peak} I (°C), T_{peak} II (°C) and T_{peak} III (°C), respectively. The maximum drying peak of the torrefied pellets occurred between 62.35 and 81.47 °C, which is lower than the raw OPEFB pellets (84.79 °C). This confirms the MC of the torrefied OPEFB pellets are lower than the raw OPEFB pellets, and hence require less thermal input for drying.

In stage II, the T_{peak} II for the raw OPEFB pellets increased by 2.84 °C for the torrefied OPEFB pellets at 250 °C but decreased by 6.82 °C and 19.16 °C for the pellets torrefied at 275 °C and 300 °C, respectively. The T_{peak} II for the raw OPEFB Pellet was higher for the torrefied OPEFB pellets at 250 °C but lower for the pellets torrefied at 275 °C and 300 °C. This could be ascribed to the lower volatile matter content and loss of hemicellulose in the torrefied pellets. Hemicellulose is the most reactive biomass component, and

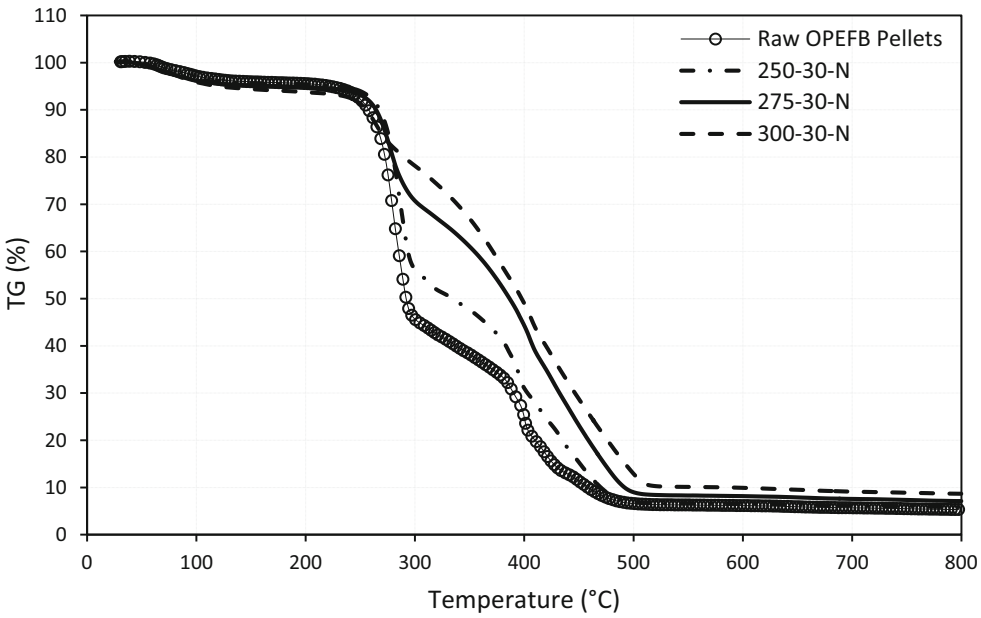

Fig. 10 TG plots for raw and torrefied OPEFB pellets

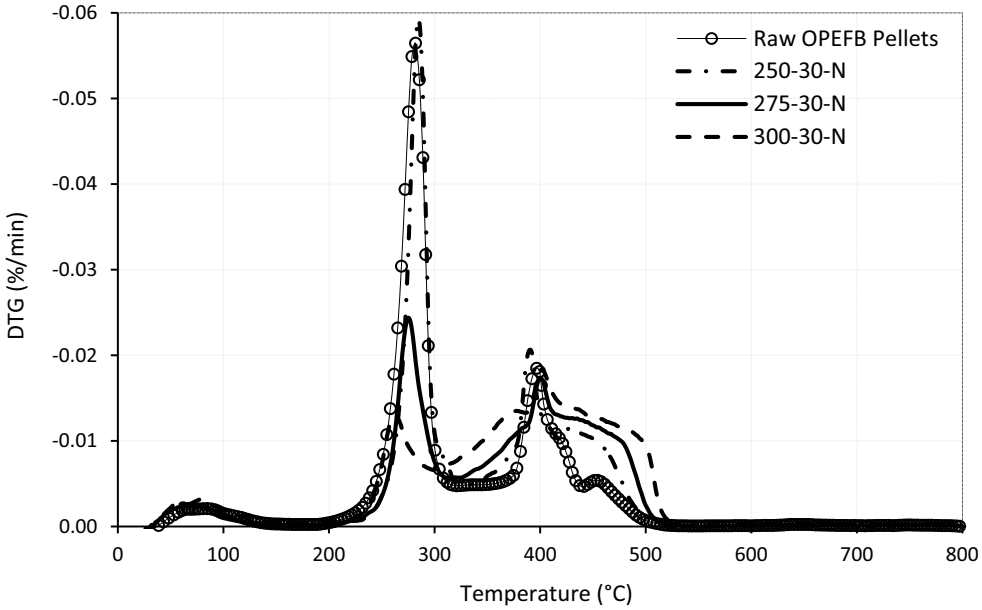

Fig. 11 DTG Plots for raw and torrefied OPEFB pellets

its degradation is considered the rate-determining step of the torrefaction process [47, 79]. The reactivity of the raw OPEFB and torrefied OPEFB pellets was also examined based on the mass-loss rates (MLR). As observed in Table 7, the MLR of the torrefied pellets were lower than the raw pellets and decreased with increasing severity of torrefaction. This confirms the torrefied OPEFB pellets are less thermally reactive compared to the raw OPEFB pellet. The decrease in reactivity could be ascribed to the lower volatile matter and increased ash and fixed carbon contents of the torrefied OPEFB pellets, as earlier presented in Table 4. The volatile matter content influences the ignitability, thermal degradation and product distribution during thermochemical conversion of biomass [24]. Lastly, stage III was characterised by a maximum decomposition peak denoted as T_{peak} III during TGA. Similarly, its values increased with increasing severity of the torrefaction, which indicates slow reactivity of the chars (evidenced by lower MLR) after devolatilization in stage I.

3.8 Torrefaction liquid properties

The torrefaction of the OPEFB pellets from 250 to 300 °C produced 19.37% to 40.09% liquid yield (products). As observed in Fig. 12, the liquid products produced different hues, which darkened progressively with increasing severity of the torrefaction temperature.

As observed, the colour for the torrefaction liquids was light brown (after torrefaction at 250 °C), dark brown (at 275 °C) and black (at 300 °C), which follows a similar trend as observed for the solid torrefied products in Fig. 5. Further analysis indicated that the colour of the liquid products darkened exuding more pungent smells with increasing severity of the torrefaction process. The liquid product after torrefaction at 300 °C (Fig. 12c) also contained significantly higher tarry compounds compared to the products at 275 °C and 250 °C in decreasing order. As observed in Fig. 12c, the torrefaction liquid consists of dark immiscible tar layer at the top of the bottle, whereas the water fraction was at the bottom. The dark hues in the tarry and turbid water fractions are due to the thermally degraded lignocellulosic (hemicellulose, cellulose and lignin) biomass components, which increases at higher temperatures during torrefaction. The presence of the compounds affects the water content and pH of the torrefaction liquid products [51, 80].

Therefore, the pH and water content were analysed to examine the effects of the tar compounds on the torrefaction liquid products (T_{LQ}). The results showed that the pH of the torrefied liquid products decreased from 3.22 after

Table 6 TG characteristics of the raw OPEFB and torrefied OPEFB pellets

Sample code/torrefaction temperature	Onset Temp. (T_{onset}, °C)	Offset temp. (T_{end}, °C)	Mass loss (M_L, %)	Residual mass (R_M, %)
OPEFB pellets	262.01	327.97	94.90	5.10
250	264.68	330.80	94.24	5.76
275	270.54	374.17	92.93	7.07
300	285.50	476.73	91.50	8.50

Table 7 DTG characteristics of the raw OPEFB and torrefied OPEFB pellets

Sample code/torrefaction temperature	Stage I	Stage II		Stage III	
	T_{peak} I (°C)	T_{peak} II (°C)	MLR (%/min)	T_{peak} III (°C)	MLR (%/min)
OPEFB pellets	84.79	282.00	31.83	396.70	8.74
250	62.35	284.84	32.19	390.39	9.16
275	69.44	275.18	12.84	400.40	7.35
300	81.47	262.84	4.70	401.62	5.70

torrefaction at 250 °C to 2.93 after torrefaction at 275 °C, and lastly 2.89 after torrefaction at 300 °C. Hence, the acidity of T_{LQ} increased with increasing severity of the torrefaction. The increase in acidity is typically ascribed to the presence of volatile, phenolic, fatty, resin, hydroxyl and other organic acid compounds collectively termed the "organics content" in the T_{LQ} [81]. The increase in torrefaction temperatures enhanced the lignocellulose degradation into the water and organic fractions as observed in the study. Similar results have been reported for the pH of the liquid products (2.27–2.60) for bamboo torrefaction from 250 to 300 °C [51]. The results are also similar to bio-oil (2.95–3.34) from corn stalk pyrolysis [80]. Next, the water and organics of the torrefaction liquids were analysed by Karl Fischer titration (KFT) as presented in Fig. 13.

As observed, the water content decreased from 67.64 to 62.62%, whereas the organics fraction increased from 32.36 to 37.38% with increasing severity of torrefaction. Hence, the findings indicate an inverse relationship between the water and organics content for the torrefaction of the OPEFB Pellets from 250 to 300 °C. The decrease in water content is due to the higher rate of drying at higher torrefaction temperatures. Likewise, higher temperatures enhanced the degradation of lignocellulosic and volatile components of the OPEFB pellets through various thermochemical reactions. The most notable are devolatilization, decarboxylation and the glycosidic C-O and C-C bond breaking reactions as described in the literature [82]. These reactions account for the high organic compounds such as acids, alcohols, aldehydes and tar [51, 83] and the acidic pH of the liquid torrefaction products as earlier reported. In general, the findings indicate that torrefaction, particularly at 300 °C, is a potential route to source green chemicals due to phenolic, resin, alcohols, aldehydes, organic acid and other tar compounds present in the liquid products (T_{LQ}).

4 Potential applications and future outlook

Global scientific interest in torrefaction has soared over the years. The growing attraction is mostly attributed to its potential utilisation as both pre-treatment and valorisation technologies for upgrading problematic biomass and its fuel properties. Numerous studies have highlighted the challenges of valorisation and energy recovery of fresh, raw or untreated biomass such as oil palm wastes (OPW). In particular, the valorisation of OPEFB is currently hampered by its high moisture, alkali and mineral matter content, ash along with low

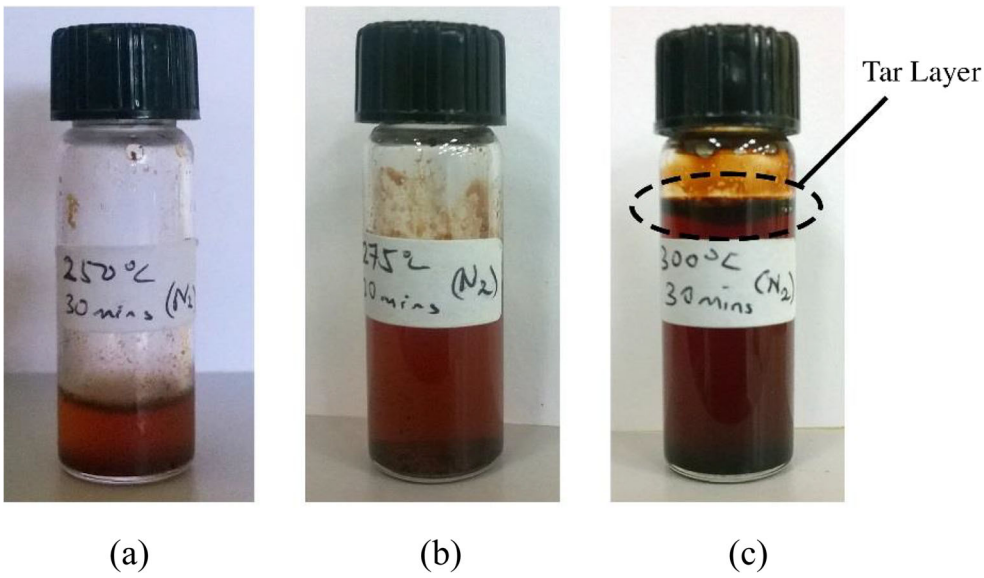

Fig. 12 Colours of liquid products after OPEFB pellets torrefaction. **a** 250 °C. **b** 275 °C. **c** 300 °C

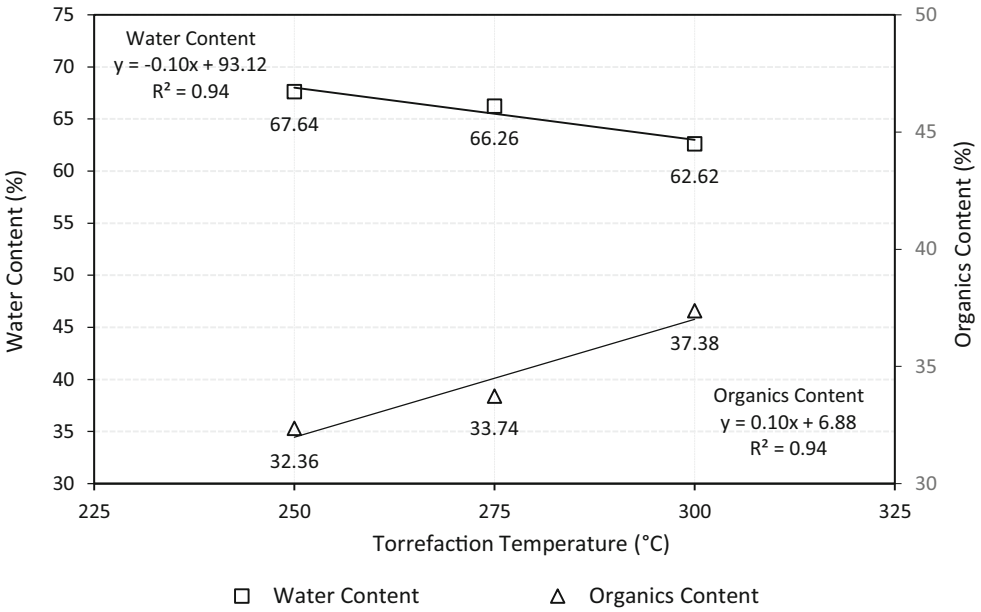

Fig. 13 Water-organics content of the torrefaction liquid products

heating values, energy density and grindability. However, it has been demonstrated that the torrefaction and pelletization of OPEFB enhance its solid fuel properties and energy recovery potential. In this study, the torrefaction of OPEFB Pellets along with the characterisation of the fuel properties, yield and distribution of products was examined in detail. The findings showed that the combined effect of pelletization and torrefaction (PET process) addresses not only the earlier outlined problems of pelletizing torrefied biomass particles (i.e. TOP process) but also produces higher quality torrefied pellets.

According to the annual Biofuels report of the United States Department of Agriculture (USDA), the global demand for wood-based Pellets is projected to exceed 30 million tonnes in 2020. The consumption of wood pellets, particularly in the largest consumer countries such as the UK, Italy, Denmark and Germany, is primarily for residential heating (~ 40%) through combined heat and power (CHP) technologies. As the world's largest wood pellets market, the European Union (EU) currently has an installed capacity of 25 million tonnes based on the capacity utilisation of 74%. Despite accounting for 30% of the global market, the production of wood pellets among the largest EU producing nations (Germany, Sweden, Latvia and others) is limited to 18.5 million, which leaves a deficit of 12.5 million [84, 85]. Likewise, there is a growing demand for biomass fuels from Japan, South Korea, India and China, which creates an expanded demand for pelletized fuels or derivatives. Furthermore, there are growing calls for stricter regulations and sustainability criteria regarding the sourcing, production, transportation and utilisation of wood-based pellets as ratified by the EU Renewable Energy Directive (RED) and European Commission (EC) by the year 2026 [86].

One potential route to address the supply shortfall and sustainability concerns is the adoption of non-woody torrefied biomass such as OPEFB pellets. Currently, the primary utilisation of wood-based pellets has severely limited the global feedstock base for pellets, thereby resulting in specification, quality, transport and usability issues [87]. Hence, the use of torrefied and pelletized biomass from non-wood sources such as OPEFB could potentially address the outlined challenges of wood pellets such as 12.5 million annual deficit. However, there are pertinent questions about the practicality and suitability of torrefied OPEFB pellets that need to be addressed. For example;

- What are the potential applications of the torrefied OPEFB pellets?
- What is the market value of the torrefied OPEFB pellets?

The findings of this study showed that torrefied OPEFB pellets has low moisture (< 5%), sulphur (< 0.14%), nitrogen (< 1.12%) and high heating values (22.83–25.81 MJ/kg) similar to sub-bituminous coal. When compared to the DIN Plus and EN Plus European standards [88], the torrefied OPEFB pellets meet the heating value (> 16.5 MJ/kg), moisture content (< 10%), length and diameter requirements. The nitrogen, sulphur and ash contents will, however, require additional conditioning before future applications. In general, the torrefied OPEFB pellets could be potentially utilised as candidate feedstock for co-firing with coal in existing power plants. For example, the 1000 MW coal-fired Tanjung Bin Energy and 624 MW coal-fired Balingian power plants located in Johor and Sarawak States in Malaysia, respectively. Incidentally, the two states have the largest oil palm plantations, palm oil wastes and processing mills, and are

hence aptly positioned to test run torrefied OPWs and coal co-firing schemes. Likewise, the IEA Bioenergy report [87] also projects that torrefied biomass could be utilised as future feedstock for pulverised coal-fired power plants along with applications in cement making ovens, mid-sized burners and biomass gasifiers [89, 90]. Other studies have predicted that torrefied biomass could even serve as a sustainable alternative to coal and other fossil fuels in utility-scale power or district heating plants or industry [91]. Alternatively, the torrefied OPEFB pellets could be exported to the EU, thereby earning extra revenue for oil palms mills and foreign exchange for the government.

The condensate (liquid and gas) torrefaction products, as reported for OPEFB pellets torrefaction in this study, could be used as biopesticides, wood varnish, plywood resins or pellet binders [90]. Typically, the condensates contain phenolic, resin, hydroxyl organic acids along with alcohols, aldehydes and other chemical species. Furthermore, the high carbon and fixed carbon contents of the torrefied OPEFB pellets indicate prospective utilisation in the synthesis of activated carbon, mesoporous adsorbents, carbon dots and carbon microspheres for water treatment, super-capacitors, batteries and energy storage. Lastly, the milder operating conditions of the torrefaction process could provide significant savings in terms of financial costs, energy and materials to manufacturers of carbonised biomass.

The outlined prospects indicate there is a huge market for torrefied biomass such as the torrefied OPEFB pellets. On the other hand, the market for torrefied biomass according to Hawkins Wright [91] has "struggled to gain a foothold in the market" over the years primarily due to issues such as the gap in the desired user demand and sustained supplies. Other issues such as the first-mover advantage enjoyed by the producers of conventional wood pellets, fuel wood and fossil fuels could also be responsible for the challenges faced by the global torrefied biomass market. Despite this, many analysts believe that with significant investments in technology, marketing and utilisation, the torrefied biomass and pellets could break even in the coming years. For example, the Hawkins Wright [91] report states that about eight planned projects (seeking permits) along with seven commercial-scale plants amounting to about 2 million tonnes are currently being constructed with commissioning dates around 2021. It has been reported that lowering the investment, and production costs as well as addressing issues related to operational capacity, and market pricing could also enhance the competitiveness of torrefaction [89]. Likewise, the torrefied OPEFB pellets as reported in this paper will require significant investments in commercialisation technologies, product marketing and large-scale utilisation projects despite its high quality, storage, transport and utilisation potentials. Hence, it is recommended that future work on the techno-economic analyses is carried out to comprehensively examine the long term prospects of torrefied OPEFB pellets since this is currently not within the scope of the current paper.

5 Conclusions

The torrefaction of oil palm empty fruit bunch (OPEFB) pellets was examined from 250 to 300 °C for 30 minutes under nitrogen (N_2) gas atmosphere. The torrefaction products were distributed among the solid mass (M_Y), liquid (L_Y) and gas (G_Y) yields. The findings revealed that the mass yield (M_Y) decreased with increasing torrefaction temperatures, whereas increasing trends were observed for the liquid (L_Y) and gas (G_Y) yields after torrefaction. The observed trends can be ascribed to drying, devolatilization and depolymerisation of lignocellulosic biomass components during torrefaction. Fuel characterisation of the solid mass (M_Y) products indicated that ultimate (elemental), proximate, HHV properties along with the energy yield (E_Y), energy density (D_E) and severity factor (S_F) were significantly transformed after torrefaction. Likewise, the torrefaction process significantly altered the microstructural, mineralogical and morphological properties of the OPEFB pellets. The dense network of fibres in the OPEFB pellets was depolymerised and defibrillated, which resulted in a highly porous and carbonaceous material with a beehive or honeycomb microstructure. The pH of the torrefied OPEFB pellets was alkaline compared to the slightly acid raw pellets. The hydrophobicity tests showed that although the structure of the raw OPEFB pellets disintegrated entirely after the 2-hour test, the torrefied OPEFB pellets showed higher resistance to water absorption. Likewise, the grindability (brittleness and friability) of the OPEFB pellets increased after torrefaction due to the degradation of the holocellulose and lignin. Thermal analysis revealed that torrefaction does not enhance the rate of thermal degradation as evident in the decreased MLR (%/min) after torrefaction. This finding indicates that higher energy input and reaction times are required to effectively or completely decompose the torrefied pellets compared to the raw pellets. Lastly, the analysis of the torrefaction liquid revealed an acidic product with organic (67.64–62.62%) and water (32.36–37.38%) fractions after torrefaction. The potential applications and future outlook on OPEFB Pellets indicate it has promising potentials as fuel for co-firing with coal in power plants, substitute to fossil fuels or feedstock material for producing other value-added products. However, these prospects are expedient on addressing the current problems faced by the global biomass pellets market. Overall, the findings indicate that torrefaction yielded a high HHV, grindable, hydrophobic and thermally stable torrefied OPEFB pellets with potential application as a solid fuel for future energy recovery, storage or other value-added products.

Acknowledgements The support of the Hydrogen and Fuel Cell Laboratory, Centre of Hydrogen Energy, and the Institute of Future Energy all at Universiti Teknologi Malaysia (UTM) Skudai Campus in Johor are all gratefully acknowledged.

References

1. Yan W (2017) A makeover for the world's most hated crop. Nature, vol 543. Springer Nature Inc., USA
2. Foong SZY, Goh CKM, Supramaniam CV, Ng DKS (2019) Input–output optimisation model for sustainable oil palm plantation development. Sustain Prod Consum 17:31–46
3. Johari A, Nyakuma BB, Nor SHM, Mat R, Hashim H, Ahmad A, Zakaria ZY, Abdullah TAT (2015) The challenges and prospects of palm oil based biodiesel in Malaysia. Energy 81:255–261
4. Taufiq-Yap Y, Farabi MA, Syazwani O, Ibrahim ML, Marliza T (2020) Sustainable Production of Bioenergy. In: Ashwani KG, Ashoke D, Suresh KA, Abhijit K, Akshai R (Eds) Innovations in Sustainable Energy and Cleaner Environment. Green Energy and Technology. pp 541–561 Springer, Singapore. https://doi.org/10.1007/978-981-13-9012-8_24
5. Cazzolla Gatti R, Liang J, Velichevskaya A, Zhou M (2019) Sustainable palm oil may not be so sustainable. Sci Total Environ 652:48–51
6. MPOB (2019) Overview of the Malaysian Oil Palm Industry 2018. Palm Oil Statistics. Malaysian Palm Oil Board, Kuala Lumpur, Malaysia
7. AIM (2013) National Biomass Strategy 2020. New wealth creation for Malaysia's palm oil industry, vol 2.0, 2nd edn. Agensi Inovasi Malaysia (AIM), Kuala Lumpur
8. Ganapathy B, Yahya A, Ibrahim N (2019) Bioremediation of palm oil mill effluent (POME) using indigenous Meyerozyma guilliermondii. Environ Sci Pollut Res 26(11):11113–11125
9. Loh SK (2017) The potential of the Malaysian oil palm biomass as a renewable energy source. Energy Convers Manag 141:285–298
10. Mahlia TMI, Ismail N, Hossain N, Silitonga AS, Shamsuddin AH (2019) Palm oil and its wastes as bioenergy sources: a comprehensive review. Environ Sci Pollut Res 26 14849–14866 (2019). https://doi.org/10.1007/s11356-019-04563-x
11. Chin K, H'ng P, Maminski M, Go W, Lee C, Raja-Nazrin R, Khoo P, Ashikin S, Halimatun I (2018) Additional additives to reduce ash related operation problems of solid biofuel from oil palm biomass upon combustion. Ind Crop Prod 123:285–295
12. Ashikin NSSN, Djalaluddin A, Yusuff S, Khalil HA, Syakir MI (2019) Empty Fruit Bunch-Seaweed Biocomposite as Potential Soil Erosion Mitigation Material for Oil Palm Plantation. BioResources 14(3):5438–5450
13. Demirbas A (2011) Waste management, waste resource facilities and waste conversion processes. Energy Convers Manag 52(2):1280–1287
14. Chiew YL, Shimada S (2013) Current state and environmental impact assessment for utilizing oil palm empty fruit bunches for fuel, fibre and fertilizer—a case study of Malaysia. Biomass Bioenergy 51:109–124
15. Krishnan Y, Bong CPC, Azman NF, Zakaria Z, Abdullah N, Ho CS, Lee CT, Hansen SB, Hara H (2017) Co-composting of palm empty fruit bunch and palm oil mill effluent: microbial diversity and potential mitigation of greenhouse gas emission. J Clean Prod 146:94–100
16. Taheripour F, Hertel TW, Ramankutty N (2019) Market-mediated responses confound policies to limit deforestation from oil palm expansion in Malaysia and Indonesia. Proc Natl Acad Sci 116(38):19193–19199
17. Uemura Y, Sellappah V, Trinh TH, Hassan S, Tanoue K-i (2017) Torrefaction of empty fruit bunches under biomass combustion gas atmosphere. Bioresour Technol 243:107–117
18. Mohammed MAA, Salmiaton A, Wan Azlina WAKG, Mohamad Amran MS (2012) Gasification of oil palm empty fruit bunches: A characterization and kinetic study. Bioresour Technol 110(0):628–636
19. Asadieraghi M, Daud WMAW (2015) In-depth investigation on thermochemical characteristics of palm oil biomasses as potential biofuel sources. J Anal Appl Pyrolysis 115:379–391
20. Nyakuma BB, Ahmad A, Johari A, Tuan TA, Oladokun O, Aminu DY (2015) Non-isothermal kinetic analysis of oil palm empty fruit bunch pellets by thermogravimetric analysis. Chem Eng Trans 45:1327–1332
21. Olugbade T, Ojo O, Mohammed T (2019) Influence of binders on combustion properties of biomass briquettes: a recent review. BioEnergy Res 12(2):241–259
22. Sukiran MA, Daud WMAW, Abnisa F, Nasrin AB, Astimar AA, Loh SK (2020) Individual torrefaction parameter enhances characteristics of torrefied empty fruit bunches. Biomass Conv Bioref. https://doi.org/10.1007/s13399-020-00804-z
23. Pathomrotsakun J, Nakason K, Kraithong W, Khemthong P, Panyapinyopol B, Pavasant P (2020) Fuel properties of biochar from torrefaction of ground coffee residue: effect of process temperature, time, and sweeping gas. Biomass Conv. Bioref 10:743–753 (2020). https://doi.org/10.1007/s13399-020-00632-1
24. Basu P (2010) Biomass gasification and pyrolysis: practical design and theory. Academic Press (Elsevier), Burlington
25. Prins MJ, Ptasinski KJ, Janssen FJ (2006) Torrefaction of wood: Part 1. Weight loss kinetics. J Anal Appl Pyrolysis 77(1):28–34
26. Arias B, Pevida C, Fermoso J, Plaza MG, Rubiera F, Pis J (2008) Influence of torrefaction on the grindability and reactivity of woody biomass. Fuel Process Technol 89(2):169–175
27. Sadaka S, Negi S (2009) Improvements of biomass physical and thermochemical characteristics via torrefaction process. Environ Prog Sustain Energy 28(3):427–434
28. Li Y, Tittmann P, Parker N, Jenkins B (2017) Economic impact of combined torrefaction and pelletization processes on forestry biomass supply. GCB Bioenergy 9(4):681–693
29. Basu P, Rao S, Dhungana A (2013) An investigation into the effect of biomass particle size on its torrefaction. Can J Chem Eng 91(3):466–474
30. Chen WH (2015) Torrefaction. In: Pandey A, Negi S, Binod P, Larroche C (eds) Pretreatment of Biomass: Processes and Technologies, vol 1. Elsevier BV, Oxford, p 261
31. Phanphanich M, Mani S (2011) Impact of torrefaction on the grindability and fuel characteristics of forest biomass. Bioresour Technol 102(2):1246–1253
32. Nunes L, Matias J, Catalão J (2014) A review on torrefied biomass pellets as a sustainable alternative to coal in power generation. Renew Sust Energ Rev 40:153–160
33. Xue J, Chellappa T, Ceylan S, Goldfarb JL (2018) Enhancing biomass+ coal Co-firing scenarios via biomass torrefaction and carbonization: case study of avocado pit biomass and Illinois No. 6 coal. Renew Energy 122:152–162
34. Lam SS, Tsang YF, Yek PNY, Liew RK, Osman MS, Peng W, Lee WH, Park Y-K (2019) Co-processing of oil palm waste and waste oil via microwave co-torrefaction: a waste reduction approach for producing solid fuel product with improved properties. Process Saf Environ Prot 128:30–35
35. Bergman PC (2005) Combined torrefaction and pelletisation: the TOP process
36. Verhoeff F, Pels J, Boersma A, Zwart R, Kiel J (2011) ECN torrefaction technology heading for demonstration. ECN, Petten

37. Rudolfsson M, Stelte W, Lestander TA (2015) Process optimization of combined biomass torrefaction and pelletization for fuel pellet production—a parametric study. Appl Energy 140:378–384
38. Manouchehrinejad M, Mani S (2018) Torrefaction after pelletization (TAP): analysis of torrefied pellet quality and co-products. Biomass Bioenergy 118:93–104
39. Gilbert P, Ryu C, Sharifi V, Swithenbank J (2009) Effect of process parameters on pelletisation of herbaceous crops. Fuel 88(8): 1491–1497
40. Sukiran MA, Abnisa F, Daud WMAW, Bakar NA, Loh SK (2017) A review of torrefaction of oil palm solid wastes for biofuel production. Energy Convers Manag 149:101–120
41. Nyakuma BB, Wong SL, Faizal HM, Hambali HU, Oladokun O, Abdullah TAT (2020) Carbon dioxide torrefaction of oil palm empty fruit bunches pellets: characterisation and optimisation by response surface methodology. Biomass Convers Biorefinery. https://doi.org/10.1007/s13399-13020-01071-13398
42. Uemura Y, Omar WN, Tsutsui T, Yusup SB (2011) Torrefaction of oil palm wastes. Fuel 90(8):2585–2591
43. Asadullah M, Adi AM, Suhada N, Malek NH, Saringat MI, Azdarpour A (2014) Optimization of palm kernel shell torrefaction to produce energy densified bio-coal. Energy Convers Manag 88: 1086–1093
44. Li M-F, Li X, Bian J, Xu J-K, Yang S, Sun R-C (2015) Influence of temperature on bamboo torrefaction under carbon dioxide atmosphere. Ind Crop Prod 76:149–157
45. Wannapeera J, Worasuwannarak N (2015) Examinations of chemical properties and pyrolysis behaviours of torrefied woody biomass prepared at the same torrefaction mass yields. J Anal Appl Pyrolysis 115:279–287
46. Ohliger A, Förster M, Kneer R (2013) Torrefaction of beechwood: a parametric study including heat of reaction and grindability. Fuel 104:607–613
47. Bridgeman T, Jones J, Shield I, Williams P (2008) Torrefaction of reed canary grass, wheat straw and willow to enhance solid fuel qualities and combustion properties. Fuel 87(6):844–856
48. Na B-I, Kim Y-H, Lim W-S, Lee S-M, Lee H-W, Lee J-W (2013) Torrefaction of oil palm mesocarp fibre and their effect on pelletizing. Biomass Bioenergy 52:159–165
49. Yue Y, Singh H, Singh B, Mani S (2017) Torrefaction of sorghum biomass to improve fuel properties. Bioresour Technol 232:372–379
50. Zheng A, Zhao Z, Chang S, Huang Z, He F, Li H (2012) Effect of torrefaction temperature on product distribution from two-staged pyrolysis of biomass. Energy Fuel 26(5):2968–2974
51. Chen W-H, Liu S-H, Juang T-T, Tsai C-M, Zhuang Y-Q (2015) Characterization of solid and liquid products from bamboo torrefaction. Appl Energy 160:829–835
52. Rajkovich S, Enders A, Hanley K, Hyland C, Zimmerman AR, Lehmann J (2012) Corn growth and nitrogen nutrition after additions of biochars with varying properties to a temperate soil. Biol Fertil Soils 48(3):271–284
53. Pimchuai A, Dutta A, Basu P (2010) Torrefaction of agriculture residue to enhance combustible properties. Energy Fuel 24(9): 4638–4645
54. Ibrahim RH, Darvell LI, Jones JM, Williams A (2013) Physicochemical characterisation of torrefied biomass. J Anal Appl Pyrolysis 103:21–30
55. Shang L, Ahrenfeldt J, Holm JK, Sanadi AR, Barsberg S, Thomsen T, Stelte W, Henriksen UB (2012) Changes of chemical and mechanical behaviour of torrefied wheat straw. Biomass Bioenergy 40:63–70
56. Nyakuma BB, Wong S, Oladokun O (2019) Non-oxidative thermal decomposition of oil palm empty fruit bunch pellets: fuel characterisation, thermogravimetric, kinetic, and thermodynamic analyses. Biomass Conv. Bioref (2019). https://doi.org/10.1007/s13399-019-00568-1
57. Chen W-H, Zhuang Y-Q, Liu S-H, Juang T-T, Tsai C-M (2016) Product characteristics from the torrefaction of oil palm fibre pellets in inert and oxidative atmospheres. Bioresour Technol 199: 367–374
58. Talero G, Rincón S, Gómez A (2019) Biomass torrefaction in a standard retort: a study on oil palm solid residues. Fuel 244:366–378
59. Faizal HM, Shamsuddin HS, Harif MHM, Hanaffi MFMA, Rahman MRA, Rahman MM, Latiff Z (2018) Torrefaction of densified mesocarp fibre and palm kernel shell. Renew Energy 122: 419-428. https://doi.org/10.1016/j.renene.2018.01.118
60. Lee J-W, Kim Y-H, Lee S-M, Lee H-W (2012) Optimizing the torrefaction of mixed softwood by response surface methodology for biomass upgrading to high energy density. Bioresour Technol 116:471–476
61. Dowling NI, Hyne JB, Brown DM (1990) Kinetics of the reaction between hydrogen and sulfur under high-temperature Claus furnace conditions. Ind Eng Chem Res 29(12):2327–2332
62. Pinto F, Gominho J, André RN, Gonçalves D, Miranda M, Varela F, Neves D, Santos J, Lourenço A, Pereira H (2017) Improvement of gasification performance of Eucalyptus globulus stumps with torrefaction and densification pre-treatments. Fuel 206:289–299
63. Asai H, Samson BK, Stephan HM, Songyikhangsuthor K, Homma K, Kiyono Y, Inoue Y, Shiraiwa T, Horie T (2009) Biochar amendment techniques for upland rice production in Northern Laos: 1. Soil physical properties, leaf SPAD and grain yield. Field Crop Res 111(1-2):81–84
64. Dias BO, Silva CA, Higashikawa FS, Roig A, Sánchez-Monedero MA (2010) Use of biochar as a bulking agent for the composting of poultry manure: effect on organic matter degradation and humification. Bioresour Technol 101(4):1239–1246
65. Thanapal SS, Chen W, Annamalai K, Carlin N, Ansley RJ, Ranjan D (2014) Carbon dioxide torrefaction of woody biomass. Energy Fuel 28(2):1147–1157
66. Poudel J, Ohm T-I, Gu JH, Shin MC, Oh SC (2017) Comparative study of torrefaction of empty fruit bunches and palm kernel shell. J Mater Cycles Waste Manag 19(2):917–927
67. Kristensen JB, Thygesen LG, Felby C, Jørgensen H, Elder T (2008) Cell-wall structural changes in wheat straw pretreated for bioethanol production. Biotechnol Biofuels 1(1):1–9
68. Chen W-H, Lu K-M, Lee W-J, Liu S-H, Lin T-C (2014) Non-oxidative and oxidative torrefaction characterization and SEM observations of fibrous and ligneous biomass. Appl Energy 114(1): 104–113
69. Enders A, Hanley K, Whitman T, Joseph S, Lehmann J (2012) Characterization of biochars to evaluate recalcitrance and agronomic performance. Bioresour Technol 114:644–653
70. Martinsen V, Alling V, Nurida N, Mulder J, Hale S, Ritz C, Rutherford D, Heikens A, Breedveld GD, Cornelissen G (2015) pH effects of the addition of three biochars to acidic Indonesian mineral soils. Soil Sci Plant Nutr 61(5):821–834
71. Ciolkosz D, Wallace R (2011) A review of torrefaction for bioenergy feedstock production. Biofuels Bioprod Biorefin 5(3): 317–329
72. Pach M, Zanzi R, Björnbom E (2002) Torrefied biomass a substitute for wood and charcoal. In: 6th Asia-Pacific International symposium on combustion and energy utilization
73. Vassilev SV, Baxter D, Andersen LK, Vassileva CG (2010) An overview of the chemical composition of biomass. Fuel 89(5): 913–933
74. Vassilev SV, Vassileva CG, Vassilev VS (2015) Advantages and disadvantages of composition and properties of biomass in comparison with coal: an overview. Fuel 158:330–350

75. Iroba KL, Baik O-D, Tabil LG (2017) Torrefaction of biomass from municipal solid waste fractions I: Temperature profiles, moisture content, energy consumption, mass yield, and thermochemical properties. Biomass Bioenergy 105:320–330
76. Fermoso J, Arias B, Plaza MG, Pevida C, Rubiera F, Pis J, García-Peña F, Casero P (2009) High-pressure co-gasification of coal with biomass and petroleum coke. Fuel Process Technol 90(7-8):926–932
77. Zhan X, Jia J, Zhou Z, Wang F (2011) Influence of blending methods on the co-gasification reactivity of petroleum coke and lignite. Energy Convers Manag 52(4):1810–1814
78. Nyakuma B, Oladokun O, Bello A (2018) Combustion kinetics of petroleum coke by isoconversional modelling. Chem Chem Technol 12(4):505–510
79. Peng J, Bi H, Sokhansanj S, Lim J (2012) A study of particle size effect on biomass torrefaction and densification. Energy Fuel 26(6): 3826–3839
80. Chen D, Mei J, Li H, Li Y, Lu M, Ma T, Ma Z (2017) Combined pretreatment with torrefaction and washing using torrefaction liquid products to yield upgraded biomass and pyrolysis products. Bioresour Technol 228:62–68
81. Oasmaa A, Elliott DC, Korhonen J (2010) Acidity of biomass fast pyrolysis bio-oils. Energy Fuel 24(12):6548–6554
82. Yang C-y, Yang X-m, Lu X-s, J-z Y, Lin W-g (2005) Pyrolysis of straw obtained from the stagewise treatment. Chin J Process Eng 5(4):383
83. Wang G, Luo Y, Deng J, Kuang J, Zhang Y (2011) Pretreatment of biomass by torrefaction. Chin Sci Bull 56(14):1442–1448
84. Voegele E (2020) EU wood pellet demand expected to increase in 2020. BBI International. https://bit.ly/2EGkr2W. Accessed 03 August 2020
85. USDA-FAS (2020) Biofuels Report. Annual Report on Biofuels. United States Department of Agriculture (USDA), Foreign Agriculture Service (FAS), Den Haag, The Netherlands
86. Szendrei K (2015) Sustainability criteria for biomass The importance of transparency, sustainability co-benefits, and trade-offs. POLIMP - JIN Climate & Sustainability, Brussels, Belgium. Available at: https://bit.ly/2VYuhmt. Accessed 20th Jul 2020
87. Wild M, Deutmeyer M (2016) Possible effects of torrefaction on biomass trade. European Commission (EC). https://bit.ly/2DkwP8t. Accessed 04 August 2020
88. Pellet Atlas (2009) Development and promotion of a transparent European Pellets Market Creation of a European real-time Pellets Atlas. European Commission. https://bit.ly/33rg726. Accessed 03 August 2020
89. Olugbade TO, Ojo OT (2020) Biomass Torrefaction for the Production of High-Grade Solid Biofuels: a Review. BioEnergy Res:1–17
90. Thrän D, Witt J, Schaubach K, Kiel J, Carbo M, Maier J, Ndibe C, Koppejan J, Alakangas E, Majer S, Schipfer F (2016) Moving torrefaction towards market introduction – Technical improvements and economic-environmental assessment along the overall torrefaction supply chain through the SECTOR project. Biomass Bioenergy 89:184–200
91. Hawkins Wright (2020) The Black Pellet Market Outlook. Hawkins Wright Limited Accessed 03 August 2020